AN ABSTRACT OF THE THESIS OF

Erik W. Miller for the degree of Master of Science in Mechanical Engineering
presented on December 15, 2010

Title: Integrated Dual Cycle Energy Recovery Using Thermoelectric Conversion and an Organic Rankine Bottoming Cycle.

Abstract approved:

Richard B. Peterson

Hot engine exhaust and industrial process exhaust represents a resource that is often rejected to the environment without further utilization. This resource is prevalent in the transportation and industrial process sectors, but stationary engine-generator systems also typically do not utilize this resource. Engine exhaust is considered high grade heat and can potentially be utilized by various approaches to produce electricity or to drive heating and cooling systems. This thesis describes a model system that employs thermoelectric conversion as a topping cycle integrated with an organic Rankine bottoming cycle for waste heat utilization. This approach is being developed to fully utilize the thermal energy contained in hot exhaust streams. This thesis investigates several system configurations each composed of a high temperature heat exchanger which extracts thermal energy for driving the thermoelectric conversion

elements and a closely integrated bottoming cycle to capture the large amount of remaining thermal energy in the exhaust stream. The models differ by how they arrange specific heat exchangers in the system. Many interacting parameters that define combined system operation are employed in the models to determine overall system performance including output power, efficiency, and total energy utilization factors. In addition, the model identifies a maximum power operating point for the combined system. That is, the model can identify the optimal amount of heat to remove from the exhaust flow to drive the thermoelectric elements for maximizing the combined cycle output. The model has been developed such that the impact of heat exchanger UA_h values, thermal resistances, and the thermoelectric figure-of-merit (ZT) can be investigated in the context of system operation. The model also has the ability to simultaneously determine the effect of each cycle design parameter on the performance of the overall system, thus giving the ability to utilize as much waste heat as possible. Key analysis results are presented showing the impact of critical design parameters on power output, system performance and inter-relationships between design parameters in governing performance.

Keywords: Waste Heat Recovery, Thermoelectric Generator, Rankine Cycle

Integrated Dual Cycle Energy Recovery Using Thermoelectric Conversion and an Organic Rankine Bottoming Cycle

by

Erik W. Miller

A THESIS

submitted to

Oregon State University

in partial fulfillment of

the requirements for the

degree of

Master of Science

Presented December 15, 2010

Commencement June 2011

Master of Science thesis of Erik W. Miller presented on December 15, 2010

APPROVED:

Major Professor, representing Mechanical Engineering

Head of the School of Mechanical Industrial and Manufacturing Engineering

---

Dean of the Graduate School

I understand that my thesis will become part of the permanent collection of Oregon State University libraries. My signature below authorizes release of my thesis to any reader upon request

---

Erik W. Miller, Author

Acknowledgements

I would first like to thank Dr. Richard Peterson for giving me the opportunity to work with him at Oregon State University. My time studying at OSU left me very well prepared for the job I always wanted. I guess I should also thank Dr. Peterson for finding me that job I always wanted.

I also must thank Dr. Terry Hendricks and Dr. Hailei Wang who were each co-authors on the papers that became my thesis. Without their guidance I would not have been able to accomplish what I did. I would have also had to write more which I had no interest in doing. Dr. Wang also went nearly three years without kicking me out of the lab. That is certainly a large accomplishment.

Thank you to Kevin Harada, Robbie Ingram-Goble and Luke Fisher who all went through the same program as me. All the hard work would not have been nearly as enjoyable or productive without you guys.

Finally, sorry to Robbie and Luke for taking your jobs.

Contributing Authors

This thesis is written with material taken largely from two published manuscripts. Both Dr. Richard Peterson and Dr. Terry Hendricks contributed to the writing and editing efforts of those works.

Dr. Peterson, Dr. Hendricks as well as Dr. Hailei Wang also assisted with advising and suggestions in the modeling effort that makes up this thesis.

TABLE OF CONTENTS

Page

TABLE OF CONTENTS (Continued)

LIST OF FIGURES

LIST OF FIGURES (Continued)

Figure Page

1. Introduction

Internal combustion engines and many industrial processes generate waste thermal energy streams that are not currently well utilized. The magnitude of this potential thermal resource is large and can be exploited by different technologies depending on the temperature range of use; which can be classified as high, moderate, or low grade. For example, in the transportation sector nationwide, considering long haul trucking and automobile operation, an estimated 12.5 quads of high grade thermal energy is exhausted to the environment without further use[1,2]. Similar engine technology is utilized in stationary power generation where a diesel engine (or a small-scale gas turbine) is employed to spin a generator for on-site electrical power generation. Considering that only approximately 25 to 30% of the fuel energy is ultimately converted to output power and the remainder is dissipated to the surroundings in the form of heat, there is substantial opportunity to utilize waste exhaust heat to produce additional power. In the industrial sector, waste heat from materials processing and other operations generate an estimated 10 quads of heat[2 - 4]. A portion of this is high grade thermal energy and is potentially recoverable to improve the overall energy efficiency of the process.

When an IC engine is operating near its design point, high-grade waste heat is generated with temperatures potentially approaching 500 ^{o}C. This thermal energy can be used for several purposes including co-generation, additional power production,

and is attractive for other applications such as supplying heat to thermodynamic cycles that produce a cooling effect (e.g. absorption cycle cooling or mechanical-based heat-to-cooling cycles)[5,6]. In order to efficiently utilize this higher grade of heat, a potential technology should employ a cycle that can operate through a range of temperatures in order to fully capture the thermal resource availability. It is also important to realize that utilizing a thermal waste source usually involves extracting the energy from a sensible fluid stream which decreases in temperature as the thermal energy is extracted from the flow. Although the ramifications of this effect are explained in the following section, this overall concept introduces the maximum power operating point into the analysis which dictates thermodynamic constraints on the conversion process.

Two approaches that have received considerable individual attention over the years for waste heat recovery are Thermoelectric Generators (TEG) and Organic Rankine Cycle (ORC) systems. The former approach has been undergoing a renewed emphasis in recent years with the current nanotechnology focus of the research community. Improving the thermoelectric (TE) figure-of-merit through nano crystalline structure manipulation, use of lower dimensional configurations, development of skutterudites and quantum well structures are all contributing toward improving the ZT factor in TE materials[7 -9,12]. For thermal energy recovery, additional considerations must be kept in mind beyond just the improvement in material performance such as cost and reliability. The use of TEGs in heat recovery applications has been a major theme in the development of the field since the 1990's [5,7, 11 - 13]. A unique practical aspect of the

TEG approach is the ability to tailor different thermoelectric material sets to the temperature range of the application.

Although ORC development in general is mature and has been applied to waste heat recovery for many years[14, 15], newer aspects in this area include the development of smaller systems with acceptable performance, working fluids with low environmental impact, and advanced mechanical and thermal components for low cost and high performance. In this latter category, scroll expander technology and microchannel based heat transfer components are poised to make an impact in this currently mature area. When applying the ORC to waste heat recovery, the temperature of use is one important consideration. The working fluid temperature in the boiler defines the cycle temperature, and although some fluids such as toluene and naphthalene can operate at temperatures exceeding 523 K (250 ^{o}C), many newer fluorocarbon-based working fluids are limited to approximately 473 K (200 ^{o}C). This, plus the additional consideration that the smaller, non-turbine-based expanders require a circulating oil lubricant (with the working fluid) limits the upper temperature range to approximately 200 ^{o}C, especially for small-scale (1 to 10 kW_e) applications. However, at these lower temperatures, ORC systems are relatively efficient and reliable.

This thesis develops the concept of combining a TEG with an ORC for thermal energy recovery. Combining these two approaches into a dual cycle system has several advantages where each system can operate in a temperature space where its strengths are exploited. For example, allowing the TEG to operate with a higher

temperature exhaust stream exploits its capability to convert high temperature heat at an acceptable efficiency. Utilizing an ORC system to both cool the TEG and to utilize remaining sensible heat in the exhaust stream permits a level of integration and performance not achievable in single cycles alone. There are various arrangements of components in the dual cycle configuration that may have performance advantages over other configurations. An initial exploratory study of two possible arrangements is conducted here. Also, the recovery of thermal energy from a sensible fluid stream necessarily brings maximum power point considerations into the analysis , which can play a determining role in the operating points of the system. This paper develops these concepts and explores the impact of various operating parameters on system performance.

2. Literature Review

The novelty in the work presented in this paper is the combination and expansion of existing technologies and methods. The concept of waste heat recovery, although not particularly old, does have a rather extensive history. Combined cycles are also not a new concept; many large scale power plants around the world employ combined cycle setups. The purpose of this section is to discuss the previous relevant work for this thesis and lay the foundation for presenting the results. Topics such as waste heat recovery, combined cycles and thermodynamic modeling are discussed.

2.1 Waste Heat Recovery

Before discussing current techniques to generate useful work from waste heat sources it is important to understand what is meant by this terminology. Waste heat typically originates from sources which would vent useful thermal energy to the surroundings; this would then be termed waste heat. Typically these sources are the rejected heat from a power cycle or industrial process. Waste heat sources, particularly on the scale discussed in this work, are limited in both temperature and quantity. The most relevant waste heat source associated with this work comes from heavy duty trucks and stationary generators and typically has a temperature between 300 and 500 ^{o}C with a mass flow rate of 0.3-0.5 kg/s [5]. The variability of this source in regards to full load/part load operation, lower temperatures and flow rates introduces complications into the analysis that have varying effects depending on which conversion strategy is employed.

Generating useful power from waste heat is the subject of much past and current research and can be accomplished using several different approaches[10, 11, 15]. Leading technologies in the field include vapor compression cycles, absorption cycles and thermoelectric generators. Each conversion approach has strengths and weaknesses when applied to waste heat recovery.

2.2 Rankine Cycles

Rankine cycles have been extensively researched and can be found in power plants fueled by a variety of sources from coal to nuclear. A simple Rankine cycle consists of only four components including a pump, boiler, turbine or expander and a condenser. Typically found in large scale power plants, turbines in Rankine cycles do not scale down well and are inefficient at low flow rates. Many technologies are in development to solve this problem, but arguably the most promising is the development of scroll expanders. Scroll expanders are based on scroll plates containing a spiral wrap in each which when brought together in a prescribed orbiting pattern produce trapped pockets of gas that expand. A common commercially available scroll compressor, operating in reverse, gives a scroll expander. Scroll expanders operate similarly to running a compressor backwards and removing work from the flow instead of adding work. The expanders developed by Peterson et al.[6] have demonstrated isentropic efficiencies high enough to make efficient Rankine cycles on the scale of 1 kW output power are possible. A typical waste heat powered Rankine cycle is shown in Fig. 1 where the Rankine boiler is a heat recovery steam generator (HRSG).

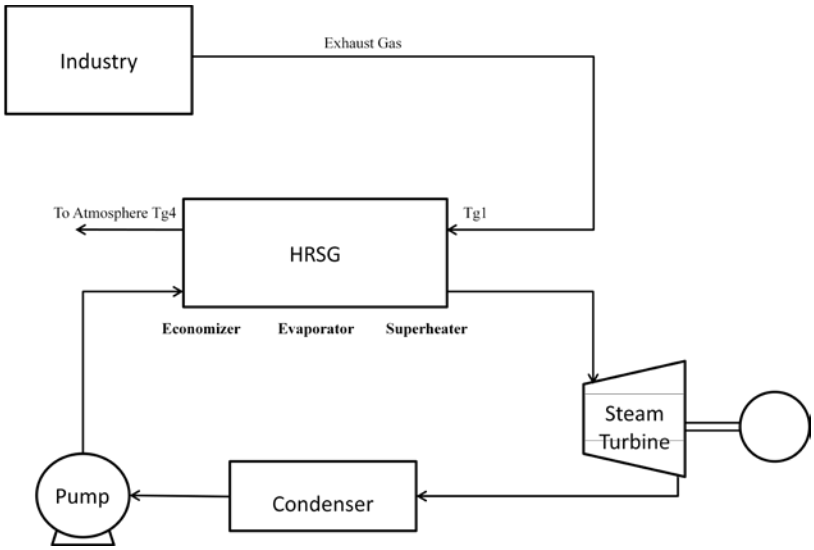

Figure 1: Vapor Compression Cycle

Figure 1 shows the setup of the Rankine cycle modeled by Butcher et al.[16] which represents the basic configuration. Several changes can be made to the simple cycle to increase cycle efficiency. Perhaps the most common improvement to the Rankine cycle is the inclusion of a recuperator, especially in systems operating with one of the so-called organic working fluids, or modern refrigerants. Typically there remains sensible heat in the working fluid after expansion. This situation exists in systems that have modest expansion ratios, or as mentioned previously, working fluids that have high internal specific heats. Instead of rejecting all the remaining sensible heat to the surroundings in the condenser, a heat exchanger is inserted between the condenser and the outlet of the expander. The hot side of the heat exchanger is the flow exiting the expander while the cold side is the flow leaving the feed pump[17]. The recuperator acts as a pre-heater before the boiler that essentially recovers still useful

heat within the cycle. The heat being used in the recupeartor would have been rejected in the condenser had a recuperator not been included.

Another possible improvement, more specific to internal combustion engine (ICE) driven waste heat cycles, is to include a pre-heater powered by the cooling flow in the ICE. Vaja et al.[18] investigated this possibility and found that the benefit to the cycle was nearly identical to the benefit of using a recuperator. It is tempting to suggest that both could be used, but this is unlikely to be possible. In either case, the heat exchanger is heating the fluid with a heat source that is only marginally warmer. This means that one heat exchanger would heat the working fluid to a temperature exceeding that of the second source, thus rendering the second source useless.

Rankine cycles work well as waste heat recovery cycles due to their ability to closely match the heat source temperature as heat is removed, leading to lower temperature differences between the two fluids and less heat rejected to the surroundings. This results in fewer irreversibilities for the cycle.[18] Fig. 2 shows a counter flow heat exchanger modeled by Butcher et al.[16] which simulates the boiler section of an ORC waste heat recovery cycle. The exhaust gas is denoted with T_g, the working fluid with T_s and the direction of flow is indicated with the arrows.

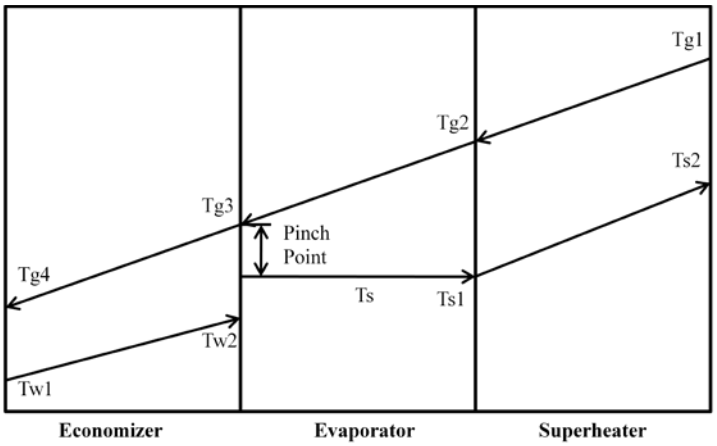

Figure 2: Boiler temperature profile

It can be seen in Fig. 2 that in this counter flow arrangement the gas side temperature is always greater than the working fluid, thereby providing the driving force for heat transfer. This arrangement removes the greatest amount of sensible heat (for a basic ORC) from the exhaust stream, but is not without complications. As is shown in Fig. 2, the phase change of the Rankine cycle working fluid creates a pinch point. That is, there is a minimum temperature difference between the hot and cold streams at a location along the heat exchanger where phase change begins. Minimizing the pinch point leads to the most effective heat exchanger performance, however careless modeling can lead to negative pinch points, which are mathematically possible but obviously physically impossible due to heat transfer considerations.

Water is often used as a working fluid in Rankine cycles where the heat source can be in excess of 1000 ^{o}C (but the working fluid remains considerably below this value), and was used in the model developed by Butcher et al.[16]. Note, however, that

water is not necessarily the best working fluid to choose for waste heat applications[17, 18]. Fluids with a lower enthalpy of vaporization will be able to match the source temperature profile of the exhaust gas more closely than that of water. This motivated Vaja et al.[18] to consider the use of Benzene, R11 and R134a in their model. Along with a lower enthalpy of vaporization, the more complex molecular structure of these working fluids tend to have overhanging vapor lines which are a benefit for expander durability. Overhanging vapor lines mean that as the fluid expands, the fluid quality will maintain its vapor characteristics and not start to condense. This is also referred to as a drying fluid upon expansion. When the quality drops below one, liquid droplets can bombard the surfaces of dynamic expanders and reduce their operating life. Scroll expanders, however, are nearly resistant to this effect.

Modeling Rankine cycles has been extensively studied and documented[16 - 20] in the past literature. One of the most important aspects of modeling a waste heat powered Rankine cycle is modeling the boiler section which represents the interaction between the heat source and the cycle itself. In nearly all approaches, the thermodynamic properties of the working fluid upon exit from the boiler are defined. There are several techniques commonly used to define how the fluid reaches the boiler exit state. All techniques ultimately use the following simplification of the first law of thermodynamics where Q is the boiler heat duty, the g subscript denotes the gas side and the R subscript represents the working fluid side.

$$Q = \dot{m}_g C_{p,g} \left(T_{g,in} - T_{g,out} \right) = \dot{m}_R \left(h_{R,in} - h_{R,out} \right) \tag{2.1}$$

The difference in the various modeling techniques is in how the individual terms in Eq. (2.1) are defined. In both cases $h_{R,out}$, $h_{r,in}$, $T_{g,in}$ and $C_{p,g}$ will be defined based on defined cycle parameters leaving the other terms to be defined. The most common method of modeling the boiler section is to define the pinch point. The boiler is normally broken into an economizer, evaporator and superheater section as shown in Fig. 2. With a defined pinch point Eq. (2.1) can be used in the three sections of the boiler to define the necessary state points [16 - 18].

More advanced models can be employed to solve Eq. (2.1) including determining the convective heat transfer coefficient for the gas side of the boiler. The heat duty of the boiler can then be defined as, Eq. 2.2 [19, 20].

$$Q = h_c \Delta T_{LMT} A \tag{2.2}$$

Another common way of defining the boiler section is using the heat exchanger effectiveness method (also referred to as the effectiveness (ε)-NTU method). This method involves calculating the maximum heat transfer rate of the hot and cold streams which is found using Eqs. (2.3) and (2.4) where h denotes the high temperature fluid, c is the low temperature fluid and the i and c represents the inlet and outlet respectively[21].

$$Q_h = \dot{m} C_{p,h} \left(T_{h,i} - T_{c,i} \right) \tag{2.3}$$

$$Q_c = \dot{m} C_{p,c} \left(T_{h,i} - T_{c,i} \right) \tag{2.4}$$

$$\dot{Q} = e C_{\min} \tag{2.5}$$

As is shown in Eqs. (2.3) and (2.4), the specific heat for each stream multiplied by the change in temperature from the hot side inlet to the cold side inlet represents the heat capacity for each stream. In heat exchangers involving phase change it is better to use enthalpy values instead as this will better account for the heat capacity involved in a phase change. Once the heat capacities are known the minimum value is used in further calculations. The minimum heat capacity is used because it sets the maximum possible heat duty for a heat exchanger. Using the maximum heat capacity will result in either the exit of the cold side being at a higher temperature than the hot side inlet or the hot side exit being colder than the cold side inlet. Obviously either of these situations is physically impossible. When the lower heat capacity is found it is multiplied by the heat exchanger effectiveness to find the heat duty of the heat exchanger. The heat duty is then inserted into Eq. (2.1) and the heat exchanger state points are defined.

After defining the boiler (and recuperator if applicable) the expander and pump are the only other complex components. Typically the pump and expander are modeled using isentropic efficiencies for those devices. Equations typically used to define the expander and pump sections are shown in Eqs. (2.6) and (2.7) where 2 denotes the component exit and 1 denotes the component inlet[22].

$$Eff_{\exp} = \frac{h_1 - h_2}{h_1 - h_{2S}} \tag{2.6}$$

$$Eff_{pump} = \frac{h_{2S} - h_1}{h_2 - h_1} \tag{2.7}$$

The 2S state in Eqs. (2.6) and (2.7) is the enthalpy of the working fluid at the component exit assuming no gain in entropy and the given pressure. Both the equation for the pump and expander are a ratio of the change in enthalpy to the change in enthalpy based on an isentropic process. An increase in enthalpy represents irreversibilities and losses in the system.

2.3 Kalina cycles

Even with advanced working fluids in Rankine cycles, constant temperature boiling is still a limiting factor. One way to eliminate constant temperature boiling is to use a Kalina cycle. Absorption power cycles use a binary mixture of two working fluids, typically water and ammonia, which allows for greater control over the boiling and condensing temperatures. Unlike either water or ammonia, a water-ammonia mixture does not boiler or condense at a constant temperature given a constant pressure. The variable temperature boiling and condensing allows the mixture to more closely follow the temperature profile of the heat source which leads to a lower temperature mismatch, and thus reduces the destruction of availability[23, 24]. As a result absorption cycles can be 10-30% more efficient than a Rankine cycle, given an identical heat source. The most prominent absorption power cycle today is the Kalina cycle which employs a mixture of ammonia and water as a working fluid.

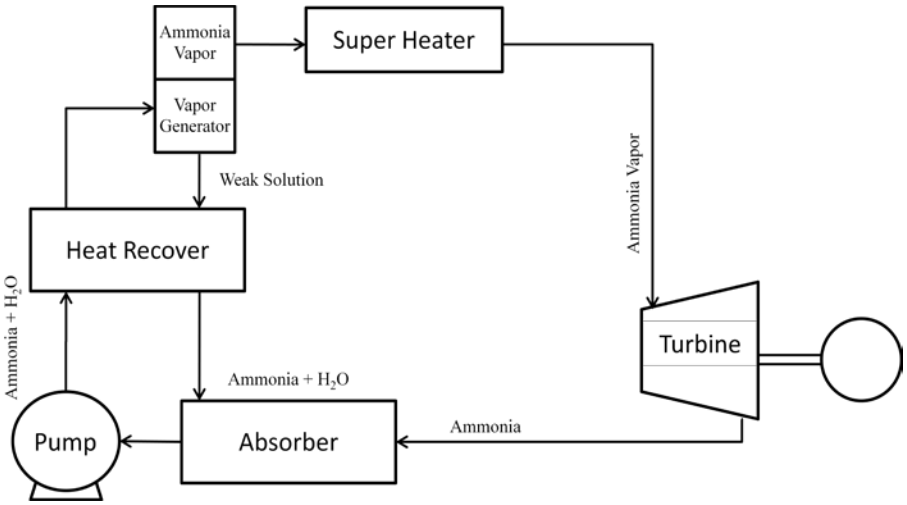

Figure 3: Kalina Cycle Diagram

The basic Kalina cycle contains the same components as the basic Rankine cycle. Like the Rankine cycle, there are several possible options for improving the Kalina cycle. A recuperator is often used to capture sensible heat from the working fluid after the expander, much like a Rankine cycle. An improvement more associated with Kalina cycles is the ability to adjust the mixture in different sections of the cycle through the use of separators and absorbers as shown in Fig. 3. Different concentrations of ammonia in water result in different thermodynamic properties that may be better for the boiler and condenser sections. Adjusting the concentration in the boiler and condenser allows for each component to be optimized[25].

Thermodynamic modeling of the Kalina cycle is more complicated than modeling a Rankine cycle because it involves more components and because correlations must be used to determine the thermodynamic properties of ammonia-water mixtures. There are many correlations that have been developed for the

thermodynamic properties of ammonia-water mixtures. Nearly all of these correlations were developed for temperatures and pressures lower than what is commonly found in power cycles, but the lower temperature of waste heat cycles allows several to be used[23]. Zhang et al.[26] used the common Peng-Robinson equation (P-R equation) to determine the thermodynamic properties of the ammonia-water mixture to accurately model a Kalina cycle. Once a correlation has been chosen, modeling a Kalina cycle is similar to modeling a Rankine cycle.

2.4 Thermoelectric Generators

Thermoelectric materials produce a voltage when exposed to a temperature gradient or produce a temperature gradient when a voltage is applied. Thermoelectric materials can be used to generate power when in the orientation where a voltage is produced from an external heat source. These are known as thermoelectric generators (TEGs). Thermoelectric generators have been studied extensively over the last 20 plus years for various applications including waste heat recovery [5,7,11,27, 28, 29, 30, 31].

Compared to Rankine or Kalina cycles, TEGs have several advantages which can make them an attractive choice for power generation. An obvious advantage of TEGs is their solid state nature where no moving parts are involved, which leads to very high reliability. Because of this, TEGs are extensively used in deep space exploration and have logged over 30 years of reliable service life. In addition to the high reliability, TEGs can more easily operate in non-steady conditions. This places

fewer restraints on the heat sources powering TEGs. Thermoelectric materials will produce a voltage when a temperature gradient is applied and maintained across the material using a heat source and cooling sink. The higher the temperature gradient the higher the voltage produced, but any temperature gradient will produce a voltage. This is particularly convenient in applications such as automotive waste heat where the temperature and quantity of heat will vary depending on driving conditions[7, 11 – 13, 29, 30].

TEGs are not without their disadvantages compared to other waste heat solutions. Like any heat engine, the performance of TEGs has a strong dependence on the temperature ratio between the hot and cold reservoirs. Unlike Rankine and Kalina cycles, TEGs do not employ a working fluid that closely matches the temperature profile of the heat source. This can lead to lower hot side temperatures and an inability to remove as much sensible heat from the heat source, although sectioned designs can overcome this to some degree. The equation governing the efficiency of TEGs is shown in Eq. (2.8) where T_{hot} is the high temperature of the TEG, T_{cold} is the cold side temperature and ZT is the figure-of-merit multiplied by the average temperature across the TEG.

$$\eta_{\max} = \frac{T_{hot} - T_{cold}}{T_{hot}} \frac{\sqrt{1+ZT} - 1}{\sqrt{1+ZT} + \frac{T_{cold}}{T_{hot}}} \tag{2.8}$$

$$ZT = \frac{S^2}{\rho\lambda} T \tag{2.9}$$

The most crippling weakness of TEGs is the figure of merit which is represented by Z in Eq. (2.9). For any thermoelectric material the figure-of-merit, Z, is strongly dependent on temperature and is typically combined with temperature to form the non-dimensional parameter, ZT, in Eq. (2.9), where T is the average of the hot and cold side temperatures in the TEG[7, 31]. As Eq. (2.8) shows, the efficiency of the TEG is also dependent on the ZT value of the material. Upon inspection of the terms in Eq. (2.9), where S is the Seebeck coefficient (VK^{-1}), ρ is the electrical resistivity (Ωm) and λ is the thermal conductivity ($Wm^{-1}K^{-1}$), it is not surprising that ZT values greater than one are difficult to achieve. As a result, temperature drops across TEGs are often over 700 K to make up for the low material ZT in order to achieve respectable conversion efficiencies. Even with a 700 K temperature drop, efficiencies in the mid single digits are common[28], however newer, advanced TE materials are beginning to increase this performance significantly [8, 9, 12].

Most current research in the field of TEGs is centered on increasing the figure-of-merit for thermoelectric materials. Improving this value through nano crystalline structure manipulation, use of lower dimensional configurations, development of skutterudites and quantum well structures are all contributing toward improving the ZT factor in TE materials[7 – 9, 11 – 13, 19, 30]. Increasing the figure-of-merit of thermoelectric materials will allow for more efficient operation and a broader range of uses for TEGs.

2.5 Combined cycle

Combined cycles employ a topping cycle which utilizes the primary heat source, and a bottoming cycle powered with the heat rejected from the topping cycle. Most of the works cited in this section are considered to be combined cycles with a diesel engine as a topping cycle. The combined cycle works well in situations where the temperature difference between the hot and cold reservoirs is larger than any one cycle can easily handle. Brayton cycles, for example, can handle combustion heat sources resulting in turbine inlet temperatures over 1500 ^{o}C but have high turbine exit temperatures as a result. Rankine cycles can reject heat at a much lower temperature, but cannot tolerate turbine inlet temperatures nearly as high as a Brayton cycle. As a result, the Carnot efficiency suffers and neither a Brayton nor a Rankine cycle can fully take advantage of a high temperature heat source. Powering one cycle using the rejected heat from the other can increase the overall temperature drop for the combined cycle and increase the overall efficiency.

Combined cycles based on diesel engines as well as combined cycles based on large-scale Brayton cycles have been the focus of much past researched. Combined Brayton and Rankine cycle work began to appear in literature in the early 1960s. By the 1970s, there were at least 40 of these types of cycles in operation in the United States, mostly in the 15-20MW range[32]. The basic combined Brayton/Rankine cycle operates much like independent versions of each cycle. The two are connected by a component usually referred to as a heat recovery steam generator (HRSG). The unit is similar to the component of the same name mentioned in the Rankine cycle section,

but instead of being powered by the exhaust of a diesel engine it is powered with the flow exiting the turbine section of a Brayton cycle. Several improvements can be made to the combined Brayton and Rankine cycle which has enabled this type of cycle to achieve thermodynamic efficiencies of 60%[33, 34]. While some common cycle improvements, such as double and triple pressure reheating, will not be effective in small scale cycles, other common combined cycle improvements are applicable on a smaller scale. Reducing the temperature difference between the hot and cold streams in the HRSG will improve cycle efficiency regardless of the cycle power output[35].

Combined cycles designed to use a primary heat source with a temperature and heat capacity on par with diesel engine exhaust have not been extensively researched. A reason for the limited development of waste heat powered combined cycles is that almost all combined cycles utilize a high temperature heat source typically generated through a combustion process. There has been some work in the field of micro-turbines (turbines with a power output of less than 200 kW) coupled with Rankine cycles, but even this scale is much larger than what can be found in a typical waste heat source. Micro turbine cycles must include recuperators and have turbine inlet and exit temperatures much lower than conventional turbines because blade cooling is not practical on that scale. As a result, the flow entering the HRSG in one of these small-scale units is much lower than a conventional large-scale combined cycle. For example, the typical turbine inlet temperature for a micro turbine is between 800 and 900 ^{o}C compared with between 1200 and 1400 ^{o}C for a conventional gas turbine. After the recuperator of a small-scale turbine, the exhaust temperature is typically 275 ^{o}C.

The low temperature of this waste heat source for driving a bottoming cycle necessitates the use of organic working fluids[17, 36, 37].

Modeling combined cycles is similar to modeling two individual cycles. Combined cycle research is dominated by Brayton / Rankine cycles and Diesel / Rankine or Kalina cycles. In both cases the two cycles are linked together by a HRSG which was discussed earlier in this section. Other than the HRSG, the two cycles are modeled as if they were independent of each other. Large scale combined cycle power plants employ more complex linking strategies, but those strategies are not viable options on a smaller scale and are thus not important to this thesis. Combined cycle systems employing cycles other than the combinations mentioned previously could be more complicated to model, but they have not been extensively researched.

3. System Configuration

3.1 Preliminary Configuration

The concept behind the dual cycle approach is that each section of the system is well suited to covert the incoming thermal energy stream at different temperatures. In the case of Fig. 4, the thermoelectric generator will operate at temperatures up to 500 ^{o}C at the hot end while rejecting heat at approximately 100 ^{o}C or lower at the cold end. Conversion efficiencies are dictated by the material ZT factor, which is assumed for the purposes of modeling in this study to be constant. The ORC cycle can operate at boiler temperatures up to approximately 200 ^{o}C (although the heat input by hot exhaust can be considerably higher) to generate power in the 12 to 15% efficiency range. When these two "cycles" are combined and allowances are made for delivering the rejected thermal energy of the TEG to the ORC cycle, it results in a system with unique and technologically useful characteristics.

In order to gain an understanding of how this dual-cycle system would operate, a brief explanation is provided with reference to Fig. 4. Hot exhaust enters the high temperature Heat Exchanger (HEX) at a temperature of T_{HHi} and leaves at T_{HHo}. Heat is delivered to the hot side of the TEG at a rate determined by the change in enthalpy of the hot stream multiplied by the mass flow rate. The actual temperature of the TEG hot side junction will be lower than T_{HHo} and is determined by using the UA_h value (explained in the next section) of the HEX and a thermal resistance. The exiting hot exhaust stream then goes on to provide heat to the boiler of the ORC system before it

is ultimately rejected to the surroundings. For the heat that passes through the TEG, a certain fraction is converted to electrical power based on the thermoelectric figure of merit; Z, and the so-called ZT factor. The heat that is rejected from the TEG cold side junction passes first through a thermal resistance and then into the working fluid of the ORC in a pre-boiler section, as shown in Fig. 4.

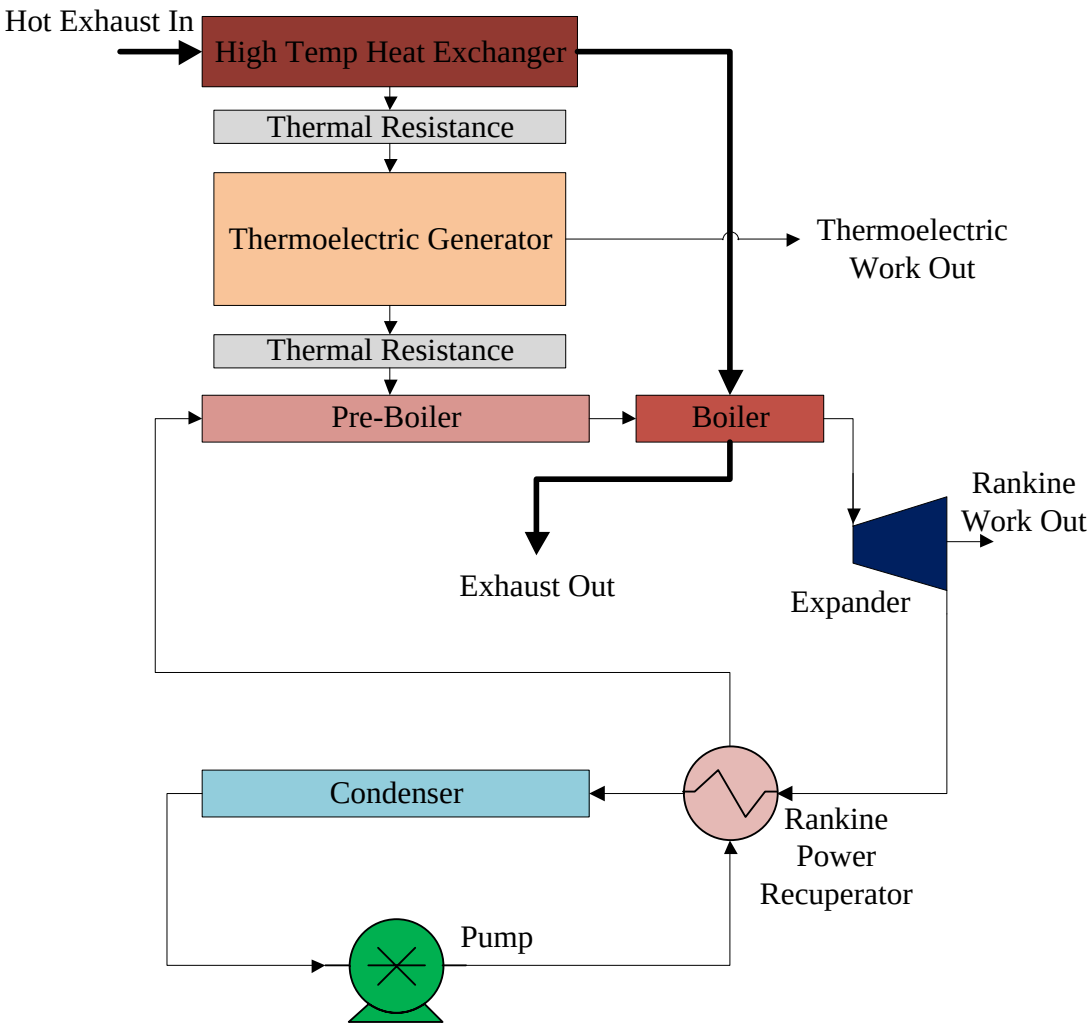

Figure 4: Schematic diagram of the dual cycle heat recovery system.

This dual cycle concept provides heat to the ORC in two separate ways. In the pre-boiler, rejection heat from the TEG is used to increase the temperature of the working fluid (after the feed pump and ORC recuperator) as the TEG cold side is cooled by this same fluid stream. If the heat load is high, the working fluid will increase in temperature to the point where partial vaporization takes place. This will

also allow high heat flux conditions to be maintained with only a small temperature difference at the TEG cold junction. Full vaporization and a small degree of super heating takes place in the ORC boiler by utilizing the other heat-containing stream exiting from the high temperature HEX. Using the TEG rejected heat to raise the enthalpy of the working fluid within this system effectively exploits the higher grade heat coming from the high temperature HEX. In this manner all the remaining exhaust heat not converted in the topping-cycle TEG is supplied to the ORC system, thereby using the total exhaust heat as effectively as possible while simultaneously "stepping down" the exhaust temperatures to be more compatible with the ORC. The output from the ORC is generated by the expander. The resulting shaft work could drive a generator to provide additional electrical power to a load or drive an appropriate cooling cycle. If thermal energy remains available in the expander exhaust, a power recuperator can be used. The anticipated working fluid for the ORC is R245fa. This dual cycle configuration tightly integrates the TEG together with the ORC so that a high utilization factor results in converting heat from the waste thermal stream to output power.

One of the fundamental thermodynamic considerations for this dual cycle is the operation at the maximum power operating point. Again with reference to Fig.4, the TEG power depends on its hot-side and cold-side temperatures, which are in turn dictated by cold-side and hot-side heat exchanger UA values as discussed in TEG system studies by Hendricks and Lustbader[5, 29, 31] and others [10, 11]. The hot-side heat exchanger UA_h also governs the hot fluid stream temperatures emerging from the heat

exchanger (T_{HHo}), which in turn impacts the ORC performance in the system. The maximum TEG power operating point is determined by the coupled performance of the hot-side and cold-side HEX and the TEG itself. This manifests itself in the TEG efficiency—power map discussed by Hendricks and Lustbader[5, 29, 31], where the maximum TEG power, maximum efficiency, and specific power tradeoffs are clearly defined. The added complexity for the dual cycle system is how this TEG–dictated operating point, its cold-side thermal dissipation, and its corresponding heat exchanger outlet temperature (T_{HHo}) influence the ORC performance and its optimum operating points.

3.2 Advanced System Configurations

Figure 5 shows a basic regenerative ORC driven by heat input from hot exhaust. This is a typical configuration used in waste heat recovery systems and it will set the baseline for comparison with dual cycles that employ thermoelectric conversion as topping cycles for an integrated approach to energy recovery. In the baseline configuration, the hot exhaust passes through the boiler where heat is removed from the exhaust stream and used to boil the working fluid in the Rankine cycle. The high pressure high temperature working fluid passes through the expander where work is produced. If the so-called organic working fluids (in actuality, these fluids have evolved from toluene and napthalene to the newer class of refrigerants) are used in the cycle, the exiting fluid from the expander still has usable energy as the expander exit temperature is typically greater than the compressed liquid temperature exiting the

pump. To achieve as high efficiency as possible, a power recuperator is used in the Rankine cycle to recover this remaining thermal energy in the expander exhaust flow. The recuperator is a counter flow heat exchanger with typical effectiveness values between 80 and 90%. As will be described in the following section, model input parameters include a wide range of operating conditions and component specifications. Pump and expander isentropic efficiencies can be specified in the model as well as boiler pinch points. For working fluid conditions, superheat ahead of the expander can be set as well as condenser saturation temperature and pressure ratio across the pump.

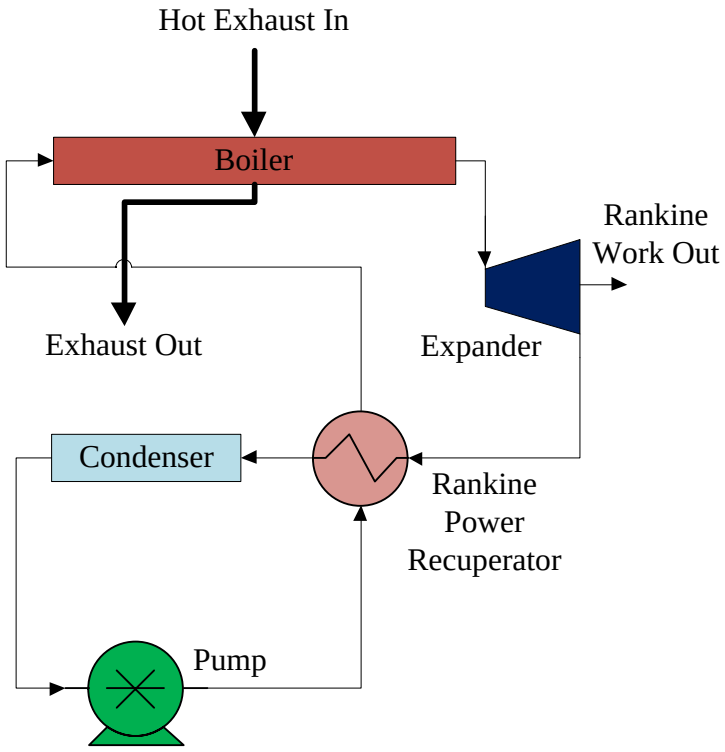

Figure 5: Schematic diagram of the Rankine cycle only configuration (RO).

The combined cycle approach joins a thermoelectric generator to a bottoming ORC for dual cycle operation. How the two sections are integrated to each other determines the thermal energy flows which ultimately impact performance. The overall concept is to allow the TEG section to convert as much of the high grade heat as possible and then use the ORC to recover the rejection heat from both the TEG and the remaining heat from the sensible fluid stream (the hot exhaust stream) after the TEG step. This fluid after passing through a high temperature heat exchanger on the TE hot-side, as shown in Fig. 5, is still hot and can be used as the heat input source for the boiler of the ORC.

It is important to extract the optimal amount of thermal energy from the exhaust stream as it passes through the high temperature heat exchanger. In order for this to take place, the heat exchanger necessarily operates at the thermodynamic maximum power point in delivering heat to the TEG. That is, if the fluid exiting the high temperature heat exchanger has a temperature only slightly below the inlet temperature, then the TEG operates at a higher conversion efficiency but little heat is sent through the TEG and thus power output is low. However, if the fluid exiting the heat exchanger approaches low values characterized by the ORC boiler temperature, the TEG operates with high levels of heat flow but at low conversion efficiency resulting in again low output. Between these two extremes there is an optimal fluid exit temperature from the high temperature heat exchanger allowing the TEG to generate maximum power yet provide substantial amounts of thermal energy to drive the bottoming ORC. Note that if this still hot exhaust stream is released to the

surroundings coming from the high temperature heat exchanger, the *total system* energy conversion efficiency would be low. This is the motivation for employing the lower temperature "bottoming" cycle to further utilize remaining thermal energy flows. Modelling considerations in this work take into account that two thermal input streams can potentially drive the ORC; i.e. rejected heat from the TEG cold side, and thermal energy remaining in the exhaust stream after passing thorough the high temperature heat exchanger on the TE hot-side.

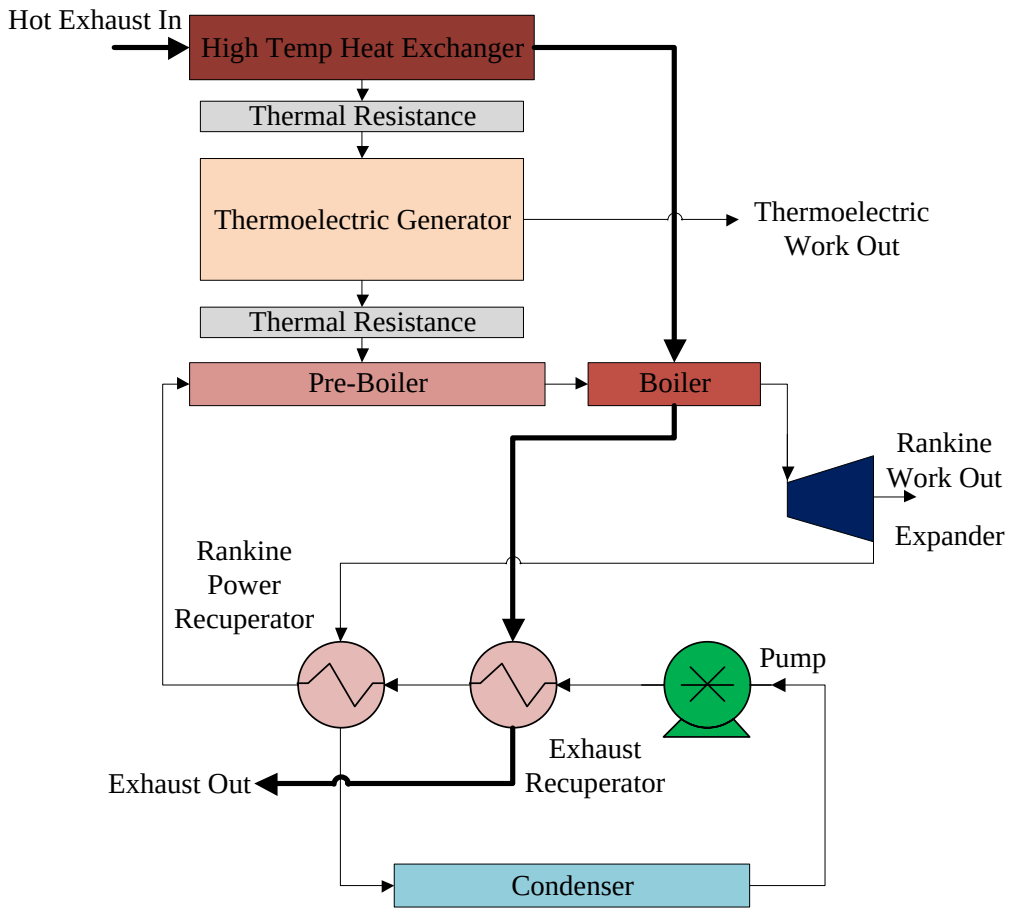

Figure 6: Schematic diagram of the Exhaust Recuperator first configuration (A1).

Combining a thermoelectric generator with a basic ORC introduces complications, but also allows opportunities to utilize residue thermal energy within the overall system. For example, thermal energy must be rejected from the cold side of the TEG elements during operation. This potentially could be accomplished by using the working fluid of the ORC, ahead of the boiler, to accomplish this cooling function. This would allow an internal system "recuperation" of the rejected heat from the TEG to pre-heat the working fluid in the ORC before the boiler. It is necessary for the

thermoelectric elements to reject heat at temperatures near ambient for efficient operation. Studies have been conducted showing the effects of rejecting heat to ambient through interface resistances characterized by air side convective heat transfer[31, 38]. This type of cooling approach for the TEG cold side has the potential to significantly raise the interface temperature and to adversely impact performance. It is proposed here that the liquid cooling of the cold side afforded by the ORC working fluid may be more effective a cooling mechanism as that provided by air side convection cooling, even after the ORC working fluid has passed through recuperation. This aspect of the integration of TEG/ORC systems is explored further in the following section.

A countervailing argument to this approach in utilizing a pre-boiler is that it reduces the ability of the boiler to extract sensible heat from the exhaust stream passing through it due to the ORC working fluid inlet temperature being higher. The higher temperature of the incoming fluid to the boiler means less heat can be taken out of the exhaust stream which leads to lower utilization of the sensible waste heat stream. A configuration consisting of a TEG topping cycle and a conventional ORC cycle integrated with a pre-boiler will be thermodynamically more efficient than an ORC alone, but less heat will be utilized because the combined cycle in this configuration cannot remove as much of the available energy from the exhaust flow.

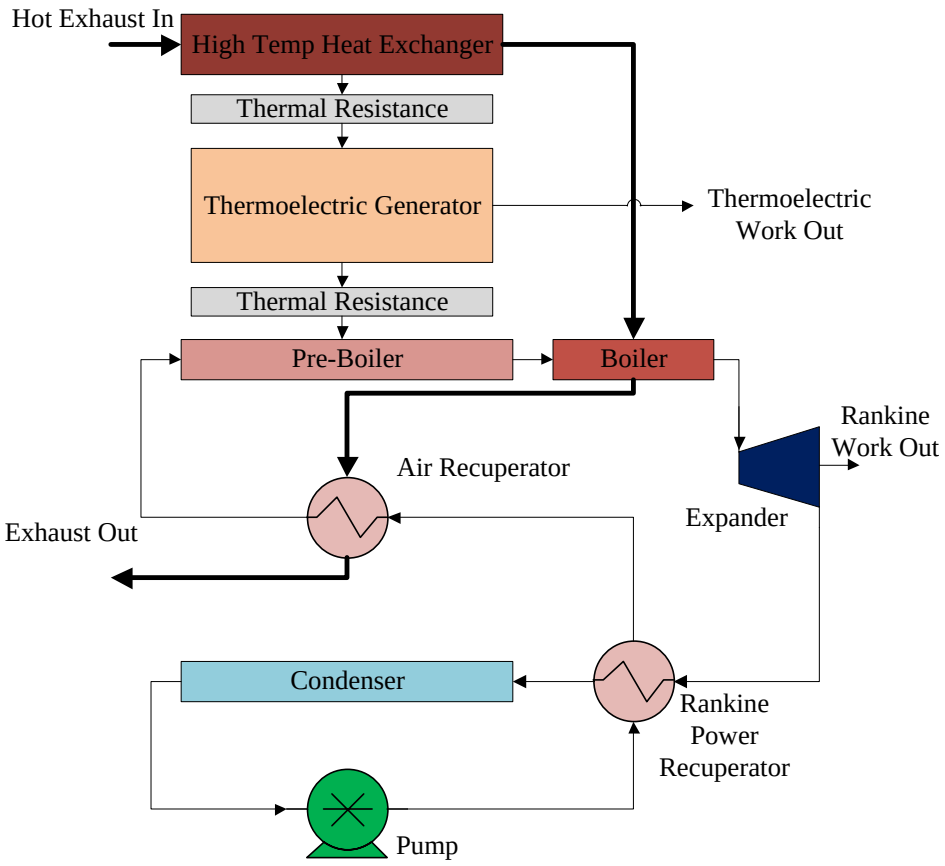

Figure 7: Schematic diagram of the Exhaust Recuperator second configuration (R1).

Because the boiler is less effective at removing heat from the sensible exhaust stream (due to the higher working fluid temperatures out of the pre-boiler), there is still a small but significant amount of heat available after the boiler. The exhaust stream can potentially pass through another heat exchanger after the boiler to remove as much exhaust heat as possible. The placement of this heat exchanger (referred to as the exhaust recuperator) was investigated and the results are discussed in the next section. Placing the exhaust recuperator as shown in Fig. 7, where the cold side inlet for the recuperator is directly after the feed pump, results in the most effective heat

transfer from the exhaust stream because the inlet temperature is the lowest. The A1 configuration shown in Fig. 6 should be capable of transferring more energy from the exhaust stream into the system because of the lower ORC temperature entering the exhaust recuperator, but the increased temperature entering the Rankine recuperator will limit the amount of heat transfer in that component. The R1 configuration shown in Fig. 7 places the exhaust recuperator after the Rankine recuperator. Switching the position of the two recuperators changes which recuperator will benefit from the lower cold side inlet temperature. As the dual cycle concept is modelled and results are analyzed, the configuration (i.e. R1 or A1) best suited for generating the maximum power output will be determined.

Another possible arrangement involves the cold side heat from the TEG being rejected to ambient air and not coupled to the ORC, i.e. no pre-boiler. The argument for this type of configuration is that forced convection of air at ambient conditions (40^{o}C in this case) could provide a lower cold side TEG temperature. A higher temperature ratio across the TEG would then increase the TEG efficiency and output power. However, the increased thermal resistance of air heat transfer compared to a liquid refrigerant heat transfer make any significant reduction in low side TEG temperature problematic. The efficiency of the TEG would have to nearly double to make up for the lost ORC work generated from heat input in the pre-boiler. A modest cold side TEG temperature drop may be achieved in this configuration, but gains in TEG performance will not make up for ORC performance reductions so this type of configuration was not investigated in this work.

4. Model Development

4.1 Preliminary Configuration

A computational model was developed for the combined TEG/ORC system using analytical expressions for the thermoelectric topping section and a thermodynamic cycle model for the bottoming portion. The model was developed using Engineering Equation Solver (EES) due to its ability to solve multiple equations with multiple unknowns using embedded function calls for the thermodynamic properties of common working fluids. Several input parameters to the model were assumed as given quantities including exhaust mass flow rate , exhaust inlet temperature, high temperature HEX characteristics, and TEG parameters (such as the ZT factor). Baseline values for these parameters, as well as others, are found in Table 1.

Describing accurately the heat flow out of the high temperature heat exchanger and into the TEG is one of the critical processes in the modeling effort. Besides the inlet and outlet temperatures to this heat exchanger, T_{HHi} and T_{HHo} , respectively, there exists an overall convective heat transfer coefficient (multiplied by the heat exchanger area) that governs the heat flow from the exhaust stream to the hot side of the TEG. This combined parameter, UA_h , provides a convective thermal conductance having the units of W/K. The parameter, through modeling equations, sets the surface temperature of the high temperature heat exchanger which directly determines (along with interface thermal resistances) the hot side temperature of the TEG. The high temperature heat exchanger is modeled as a single-fluid, single-phase, constant-

temperature heat sink due to the exhaust stream being the only fluid passing through the component. If the inlet and outlet temperatures of the exhaust stream are known, then the surface temperature of the heat exchanger is given by

$$T_{HHs} = \frac{T_{HHo} - T_{HHi} EXPHH}{1 - EXPHH} \tag{4.1}$$

where

$$EXPHH = \exp\left[\frac{-UA}{\dot{m}_{exhaust} Cp_{Tave}}\right] \tag{4.2}$$

Any real system would also have a thermal resistance between the heat exchanger and the high temperature side of the TEG. This thermal resistance would take into account conduction, thermal contact resistance, and other heat transfer effects as the heat flows from the heat exchanger to the elements of the TEG. In this model, a set thermal resistance is included between the heat exchanger and the high temperature side of the TEG, as well as between the low side of the TEG and the pre-boiler. These resistances produce a relatively modest temperature drop compared to the *UA* value mentioned above. The temperature drop across the thermal resistance is defined as

$$\Delta T_H = R_H Q_H \tag{4.3}$$

The performance characteristics of the TEG, like any other heat engine, rely on both the high side temperature, T_H , and the cold side temperature, T_C. The cold side TEG junction temperature in the computational model is dependent on the rate of heat transferred through the TEG and into the working fluid of the ORC. Because of this,

the solution process is coupled to the ORC analysis to determine the efficiency, power generated, and the heat rejected by the TEG.

The governing equations for the TEG can originate from making one of two a priori assumptions for this analysis: Efficiency can be based upon the thermoelectric elements operating at their maximum power point, or their maximum efficiency point[39, 40]. For a geometrically optimized converter operating at its maximum efficiency, where T_H is the temperature characterizing the heat input to the TEG element and M_{opt} is a simplifying term containing the figure-of-merit, *Z*, the maximum efficiency takes the form

$$Eff_{TEG} = \left[\frac{T_H - T_C}{T_H}\right]\left[\frac{M_{opt} - 1}{M_{opt} + \frac{T_C}{T_H}}\right] \tag{4.4}$$

where

$$M_{opt} = \left[1 + Z\frac{\left(T_H + T_C\right)}{2}\right]^{1/2} \tag{4.5}$$

Note that ZT_{ave} is a characteristic non-dimensional parameter of the TEG element and essentially governs its internal conversion efficiency. It is well known that the value of *Z* can have strong variations in temperature [5,7-12, 31]. In this work, in order to gain insight into optimal *system* behavior the value of ZT_{ave} is assumed constant. Little impact from this assumption is expected as the actual average temperature remains

nearly constant and temperature behavior of Z is similar in temperature ranges of interest.

Conservation of energy is used in the model to determine power generated by, and the heat flow into and out of, the TEG. The efficiency expression of Eq. (4.4) is also used for these computations. The two equations defining this connection are given by,

$$W_{TEG} = Q_H - Q_L \tag{4.6}$$

$$W_{TEG} = Eff_{TEG} Q_H \tag{4.7}$$

The two sections of the dual-cycle system are integrated together in two places. First, the cold side of the TEG rejects heat to the working fluid of the ORC through the pre-boiler. The model for this component consists of a thermal resistance for the heat flow such that,

$$\Delta T_L = Q_L R_L \tag{4.8}$$

where R_L is the low temperature side thermal resistance. And, the thermodynamic energy balance on the pre-boiler yields the state of the ORC working fluid emerging from the component. The heat input to the pre-boiler, Q_L, is removed by the liquid working fluid passing through internal channels of this heat exchange component. Since the liquid-phase heat transfer rate (and associated convection coefficient) is much higher than for a gas-phase heat transfer processes, the *UA* value at the cold heat rejection side of the TEG is assumed to be high enough that little temperature drop is present in the pre-boiler. The heat then passes into the ORC working fluid and raises the enthalpy of the flow such that

$$Q_L = \dot{m}_r \left[h_{PB,e} - h_{PB,i} \right] \tag{4.9}$$

The heat rejection temperature of the pre-boiler is based on the corresponding temperature at the enthalpy $h_{PB,e}$ (found through a thermodynamic function call for the properties of the working fluid at the value of $h_{PB,e}$).

The second location where the two sections of the dual-cycle system are integrated together is in the boiler of the ORC. Based on an energy balance on the boiler, the enthalpy of the Rankine cycle working fluid is further increased by the remaining heat flow from the waste heat exhaust stream (modeled as air) exiting the HEX (TEG hot-side heat exchanger). The mass flow rate of the Rankine cycle is set to ensure slightly superheated conditions emerging from the boiler by assigning $h_{B,e}$ to the appropriate thermodynamic state point. The energy balance on the boiler is

$$\dot{m}_h \left[h_{HHo} - h_{exh} \right] = \dot{m}_r \left[h_{B,e} - h_{PB,e} \right] \tag{4.10}$$

Included in the boiler energy transfer calculations, as well as the other heat exchange elements in the system, is the concept of heat exchanger effectiveness. There is a theoretical maximum rate of heat transfer in a heat exchanger based on the heat capacity of the two streams. In a counter-flow heat exchanger the heat capacities of the two streams are given by the following:

$$\begin{aligned} C_H &= \dot{m}_r \left[h_{h,i} - h_{T=Tci,P=Phi} \right] \\ C_C &= \dot{m}_r \left[h_{T=Thi,P=Pci} - h_{c,i} \right] \end{aligned} \tag{4.11}$$

Where $h_{T=Tci,\ P=Phi}$ is the enthalpy of the working fluid at the cold side inlet temperature and hot side inlet pressure and $h_{T=Thi,\ Pci}$ is the enthalpy of the working fluid at the hot side inlet temperature and the cold side inlet pressure.

The minimum heat capacity between the hot and cold streams is the maximum possible heat transfer rate for that device. In this work, the minimum heat capacity multiplied by the component effectiveness is the heat duty for each heat exchange device with exception of the Rankine recuperator. In the Rankine recuperator the device pinch point is important.

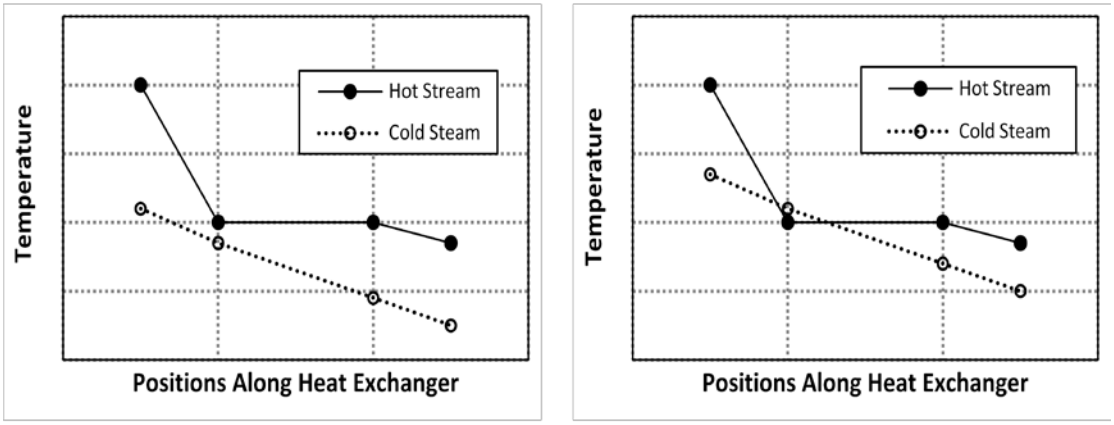

(A) (B)

Figure 8: Example Temperature Profile Along Counter Flow Recuperator

Figure 8 describes two mathematically possible temperature distributions for a counter-flow heat exchanger such as the Rankine recuperator in this thesis. The hot side is denoted with the dark circular markers and the cold side with the light markers. In this fictitious heat exchanger the hot side fluid is clearly going through a phase change which creates a pinch point. While both temperature distributions shown in

Fig. 8(a) and 8(b) are mathematically possible according to Eq. (4.10), only the distribution in 8a is physically possible. There must be a driving force for heat transfer which means that in no place along the heat exchanger can the cold side be warmer than the hot side. In the case of Fig. 8(b), the method of minimum heat capacity is not appropriate.

In cases where heat transfer laws would be potentially violated, such as the case of Fig 8(b), a more conservative approach is used. In these cases the maximum possible rate of heat transfer is given in Eq. (4.12) where $h_{P=Phi,\ Quality\ =1}$ is the enthalpy of the working fluid at the hot side inlet pressure and a quality of one.

$$C_h = \dot{m}_r \left[h_{h,i} - h_{P=Phi,Quality=1} \right] \tag{4.12}$$

The boiler, Rankine recuperator and the air recuperator (discussed later) are all modeled with care taken to assure no heat transfer laws are violated.

The analyses of the other components in the ORC are straightforward applications of the first law of thermodynamics. The expander can be described as follows where $h_{o,s}$ is the expander exit enthalpy based on isentropic expansion:

$$\begin{aligned} Eff_{\exp} &= \frac{\left[h_i - h_o \right]}{\left[h_i - h_{o,s} \right]} \\ \dot{W}_{\exp} &= \dot{m} \left[h_i - h_o \right] \end{aligned} \tag{4.13}$$

Analysis of the pump is very similar to that of the expander and is described by the equations below:

$$Eff_{pump} = \frac{\left[h_{os} - h_i\right]}{\left[h_o - h_i\right]}$$
$$\dot{W}_{pump} = \dot{m}\left[h_o - h_i\right] \tag{4.14}$$

The only component yet to be described is the condenser. The condenser is described as follows:

$$Q_{cond} = \dot{m}_r \left[h_i - h_o\right] \tag{4.15}$$

For a computational run, given the high temperature heat exchanger inlet and exit temperatures along with UA_h and ZT_{ave} values, the TEG and Rankine cycle power, efficiency and amount of heat rejected from the TEG can be found using the above described approach.

4.2 Rankine Only Configuration

Simple modifications are made to the code to describe the Rankine only cycle. Sections describing the TEG section and the pre-boiler are removed. The exhaust flows directly into the boiler which is modeled in the same way as before. Because the working fluid does not first flow through the high temperature heat exchanger the air side boiler inlet temperature is higher than in the combined cycle case. The cold side boiler inlet is colder because the Rankine working fluid has not passed though the pre-boiler. All other aspects of the Rankine cycle only configuration are the same as the combined cycle configuration.

4.3 Rankine Recuperator / Exhaust Recuperator Placement

Both the R1 Fig. 7 and A1 Fig. 6 configurations require one additional heat exchanger known as the air recuperator. The only difference between the R1 and A1 configuration is the placement of this new heat exchanger in relation to the Rankine recuperator. In the R1 configuration the working fluid flows from the pump directly into the Rankine recuperator and then the air recuperator. In the A1 configuration, the placement of the two recuperators is reversed. This new recuperator is modeled in the same way as the Rankine recuperator.

5. Modeling Results and Discussion

5.1 Preliminary Configuration

The results for the dual cycle system are presented for an averaged ZT_{ave} of 0.85. This value was chosen based on a nominal temperature difference across the TEG of 135 K with a T_H of 565 K, although temperatures for the hot and cold sides of the TEG will vary somewhat for different operating conditions. For these conditions the ZT_{ave} values for p-TAGS and n-type PbTe are 0.834 and 0.893, respectively. A value of 0.85 was chosen for the computational runs. As an introduction to the overall system characteristics for the dual cycle configuration, Fig. 9 presents the system output in kW as a function of temperature exiting the hot side heat exchanger, or T_{HHo}. By sweeping the heat exchanger exit temperature from values close to T_{HHi} to values approaching the saturation temperature of the ORC working fluid in the boiler, the maximum power operating point for the system can be found. Fig. 9 provides the two cases for UA_h values of 300 and 200 W/K. The figure shows three curves for each case representing the Rankine cycle output, the TEG output, and the combined system output. The ORC has an expander and pump efficiency of 75% and 50%, respectively, and the recuperator effectiveness has been set to 75%. These are representative values for practical systems. Further set points and baseline parameters are shown in Table 1.

Table 1: Baseline Parameters For Preliminary Configuration

Model Parameter	**Value**	**Range if Varied**
Inlet Temperature	773 K (500 ^{o}C)	–
Air Mass Flow Rate	0.25 kg/s	–
Outlet Temperature	693 K (420 ^{o}C typical)	from 320 ^{o}C to 500 ^{o}C
Average ZT	0.85 (typical)	from 0.25 to 2.0
UA_h (high temperature side)	200 W/K	from 150 to 300
Thermal Resistance (T_H side)	0.0015 K/W	–
Thermal Resistance (T_C side)	0.0015 K/W	–
Rankine Cycle Fluid	R245fa	–
Condenser Temperature	333 K (60 ^{o}C)	–
Condenser Pressure	463 kPa	–
Expander Inlet Temperature	435 K (161.6 ^{o}C)	–
Boiler Pressure	3475 kPa	–
T_{sat} at Boiler Pressure	425 K (151.6 ^{o}C)	
Feed Pump Pressure Ratio	7.5	–
Power Recuperator Effectiveness	75%	–
Expander Efficiency	75%	–
Feed Pump Efficiency	50%	–
Rankine Cycle Mass Flow Rate	0.443 kg/s (typical)	Note: will vary some

For each figure, the performance of the ORC remains relatively flat as T_{HHo} is swept throughout its range. There is slightly higher performance at the lower

temperature end, but the output remains close to 12 kW. The output from the TEG is markedly influenced by the UA_h hot side values. For a UA_h equal to 300 W/K, the TEG output remains positive and has a broad plateau with a maxima near 420 ^oC (693 K) for T_{HHo}. The output attains approximately 1.5 kW for the conditions listed. For the lower UA_h case of 200 W/K, a narrower range of temperatures, starting at 370 ^oC, gives positive output values from the TEG. In addition, the output at the maximum power point is approximately 1.1 kW. This maximum output occurs at a T_{HHo} of between 420 and 430 ^oC, which is consistent with the value of T_{HHo} = 430 °C near the maximum power point in Fig. 9(a) using the curve for a T_{cold} of 420 K. What is important here is that the ORC performance is relatively insensitive to T_{HHo}, while the TEG performance is sensitive to T_{HHo}. Therefore, one can focus on optimizing TEG performance in determining T_{HHo} in overall system-level operation.

When both the TEG and ORC outputs are combined to give a total system output, the TEG provides significant additional output especially near the maximum power output point. For the UA_h = 300 case, this operating point is near 420 ^oC and exceeds 13 kW of power output. For the UA_h = 200 case, this occurs at a T_{HHo} of 425 ^oC with an output of slightly less than the UA_h = 300 case. As the magnitude of UA_h decreases, a significant region develops where the TEG is actually degrading system performance by reducing the output from the ORC. This demonstrates the importance of maintaining high UA_h values for heat addition to the TEG portion of the dual cycle.

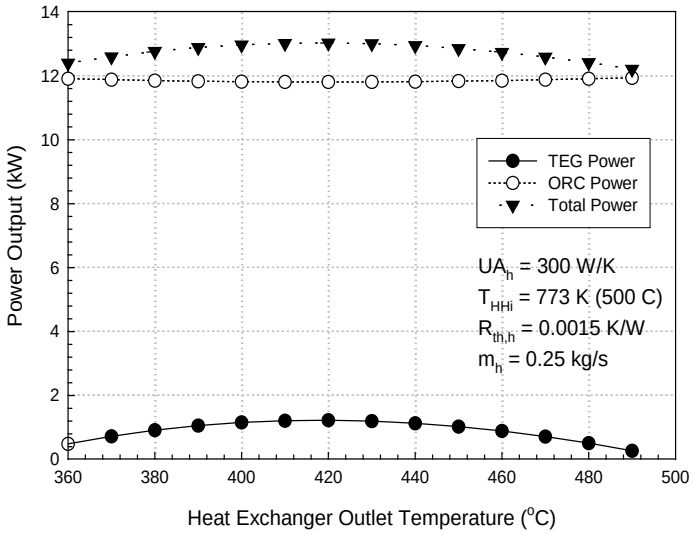

(a)

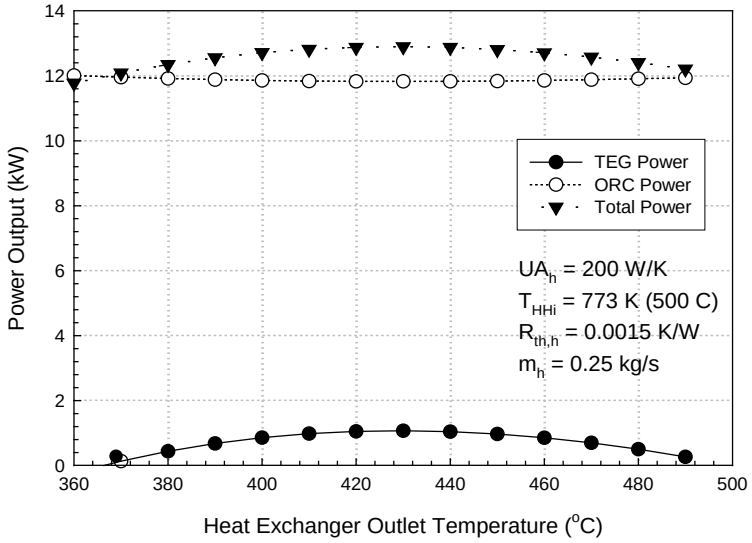

(b)

Figure 9: Dual cycle power output as a function of HEX outlet temperature

Fig. 10 displays the overall system efficiency as a function of T_{HHo} and UA_h. From this figure it is evident that UA_h values in the range from 150 to 300 W/^oC have a strong effect on the system output and efficiency, but above about 300 W/^oC, the resulting effect has diminishing further gain. For the system modeled, it would be important to design the hot side heat exchanger with a UA_h higher than 250 W/^oC and operate the system such that the exiting heat exchanger temperature was near 400 ^oC. This T_{HHO} could be varied significantly for the higher UA_h quantities due to the broad and relatively flat region in the curves. The lower UA_h values are not as forgiving for off design operating points. Note that as T_{HHo} increases toward 500 ^oC, the relative influence of UA_h on the system efficiency diminishes. This is due to a smaller fraction of system output being produced by the TEG and hence reducing the influence of UA_h on system performance. When T_{HHo} shifts toward lower temperatures, UA_h values have a greater influence on system performance.

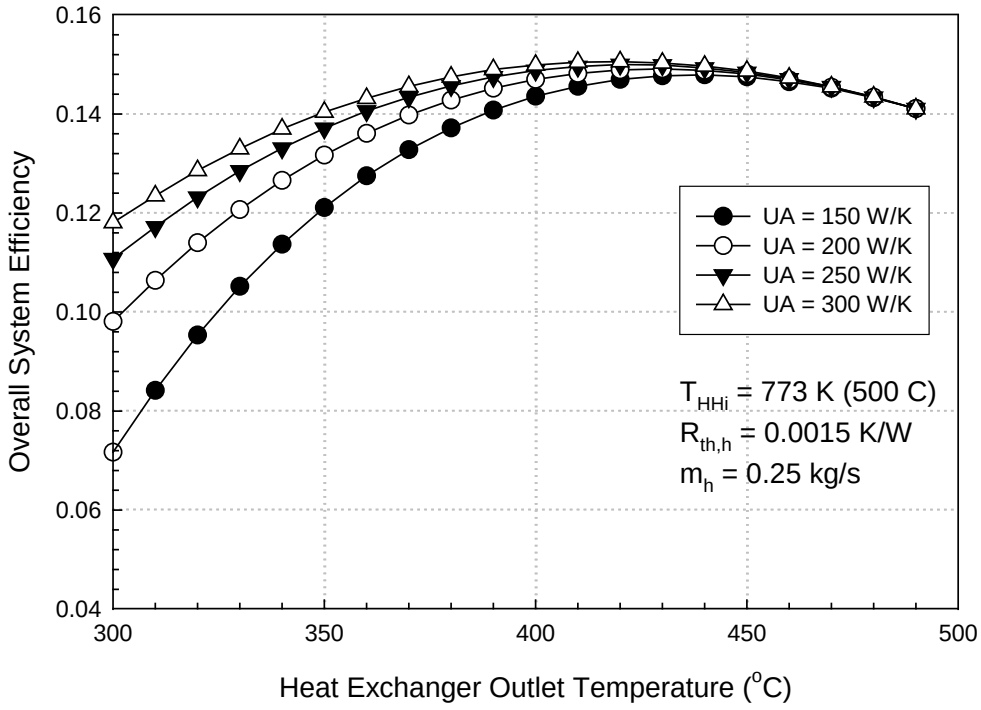

Figure 10: Total system efficiency for the dual cycle as a function of exit temperature from the high temperature heat exchanger for UAh values of 150, 200, 250, and 300 W/K.

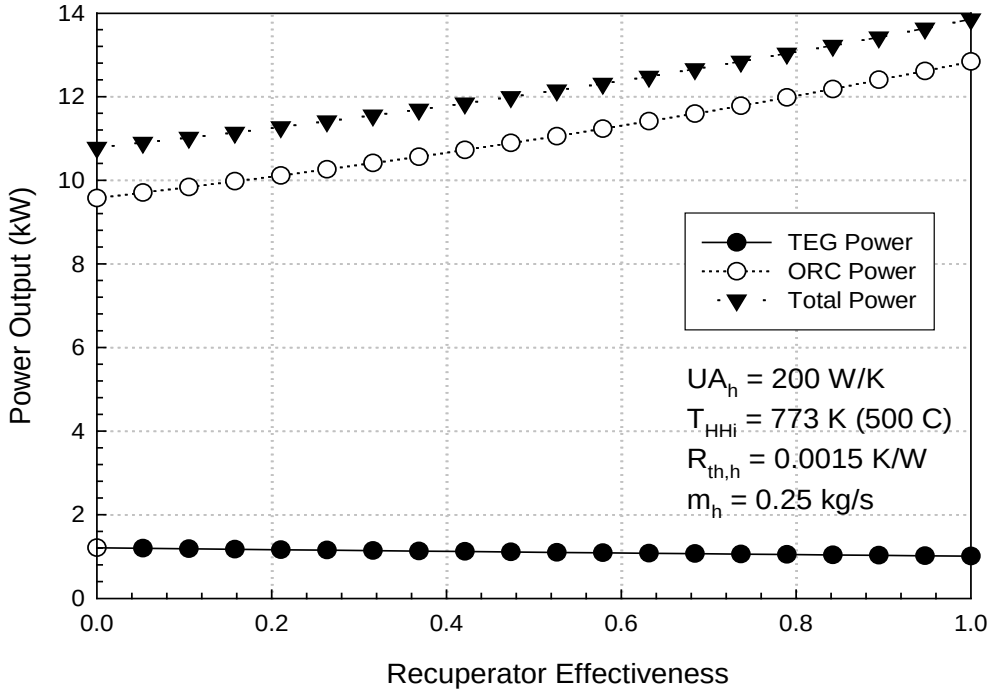

Figure 11: System power output as a function of recuperator effectiveness for a UAh value of 200 W/K and a THHo of 420 ^{o}C.

A power recuperator was used in the ORC portion of the dual cycle for increasing the performance of the system. It is not evident at first whether this component would enhance or degrade the overall performance. The recuperator recovers a portion of the thermal energy remaining in the expander exhaust and makes it available to preheat the ORC working fluid after the feed pump. On this basis, the recuperator would increase the overall power output and efficiency of the ORC. However, since the working fluid being preheated by the recuperator will increase in temperature, and hence increase the temperature at which the TEG rejects heat, this would imply a decrease in TEG performance and perhaps overall cycle efficiency as well. Figure 11

shows the result of computational runs to determine the effect of the recuperator on power output. Power output is plotted as a function of recuperator effectiveness. This latter quantity is a measure of how effective the recuperator recovers thermal energy with a value of 1.0 giving the theoretical maximum. An intermediate UA_h value of 200 W/K was used for the computations along with an average ZT_{ave} of 0.85. Also, the other baseline values for the dual cycle shown in Table1 were used. From the figure, although the TEG power output slightly decreases as the recuperator effectiveness increases, the ORC output markedly improves resulting in better overall system output. Furthermore, this output increases throughout the range of possible recuperator effectiveness values. Hence, it is important in the dual cycle configuration where an ORC is utilized to provide for the highest recuperator effectiveness as is practical. The only caveat here is that high effectiveness is typically associated with higher required heat transfer surface area or techniques to produce higher heat transfer coeffcients , which can be elaborate and impractical to implement or create undesirable cost penalties in some applications.

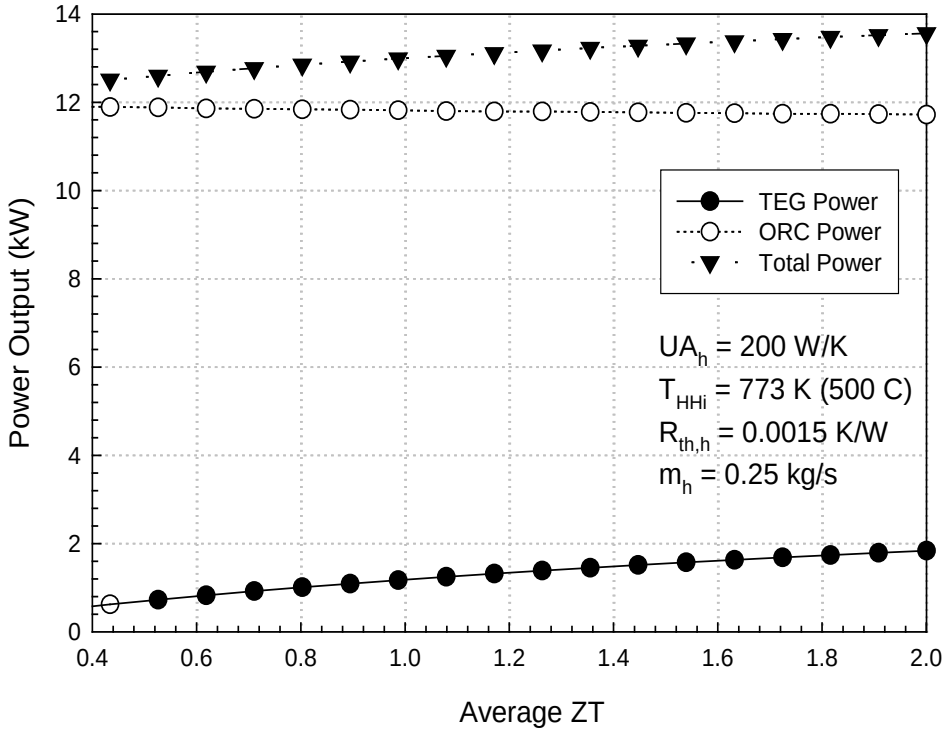

Figure 12: System power output as a function of thermoelectric figure-of-merit ZT for a UAh value of 200 W/K, a THHo of 420 ^{o}C, and a recuperator effectiveness of 0.75.

The performance of the dual-cycle system with higher ZT materials has important ramifications as the field progresses. Figure 12 displays power output as a function of average ZT for the overall cycle as well as for the TEG and Rankine sections alone. The curves show marked improvement in the TEG output as ZT increases as would be expected for higher performing TE materials. There is a corresponding slight decrease in the Rankine cycle output due to the additional power output generated by the TEG and therefore less thermal energy transferred to the ORC. The results shown in Fig. 12 were for a recuperator effectiveness of 0.75 and a hot side heat exchanger UA_h = 200 W/K. Both of these quantities could be improved beyond the baseline case to

enhance the overall performance of an advanced dual-cycle system. It should be noted that increasing the average ZT for the material would require a re-optimization of T_{HHo}.

For the dual-cycle system described here, it should be noted that the primary power output from each section of the dual cycle is fundamentally different, i.e. the TEG generates direct electrical power while the ORC produces shaft power. The latter can be converted into electrical power by way of a generator. Another approach would be to couple the shaft power to a compressor of a vapor compression cooling system. This would be especially useful in transportation applications where air conditioning is routinely needed in automobiles and long-haul trucking. To estimate the magnitude of the cooling capacity, the curve for the ORC cycle output from Fig.12 is approximately 12 kW. Conservatively estimating the range of COP for a vapor compression cooling system between 2 and 3 for vehicle conditions and duty, this implies a cooling capacity of between 24 and 36 kW. This would be a useful source of cooling for transportation-based applications.

5.2 Advanced System Configurations

Table 2 shows the state points and other model parameters defining the baseline case for the advanced combined cycle analysis. The air mass flow rate was chosen to approximately represent the exhaust flow from a moderate sized IC engine, while the heat exchanger inlet temperature was set to a higher temperature than is expected from

an exhaust stream (although temperatures more inline with IC engine exhaust are explored during the parameter variation studies). The condenser temperature is set relatively high in the baseline case (60 ^{o}C, or 333 K) to represent operation of the system on the hotter days of the year. The maximum expected ambient temperature is 49 ^{o}C (322 K, or ~120 ^{o}F), so the condenser temperature was set to achieve at least an 11 ^{o}C temperature increases over the ambient temperature to provide the driving force for heat transfer. The system would be expected to perform better during times when more moderate outdoor temperatures exist. Device effectiveness and efficiencies were chosen to reflect the current state of the art in microchannel heat transfer components and scroll expander technology.

Table 2: Baseline Case for Computational Model

Model Parameter	Value	Range if Varied
Inlet Temperature	873 K (600 ^{o}C)	–
Air Mass Flow Rate	0.5 kg/s	–
Heat Exchanger Outlet Temperature	808 K (535 ^{o}C typical)	from 753 K to 873 K
Average ZT	1.5 (typical)	from 0.25 to 2.0
UA_h (high temperature side)	300 W/K	–
Thermal Resistance (T_H side)	0.0015 K/W	–
Thermal Resistance (T_C side)	0.0015 K/W	–
Rankine Cycle Fluid	R245fa	–
Condenser Temperature	333 K (60 ^{o}C)	–
Condenser Pressure	462 kPa	–
Expander Inlet Temperature	402.6 K (129.6 ^{o}C)	from T_{sat} + 0 to T_{sat} + 40
Boiler Pressure	2310 kPa	–
T_{sat} at Boiler Pressure	402.6 K (129.6 ^{o}C)	–
Air Exit Temp of Boiler	419.6 K (146.6 ^{o}C)	
Feed Pump Pressure Ratio	5	from 4 to 7.7
Rankine Power Recuperator Eff.	80%	–
Exhaust Power Recuperator Eff.	80%	–
Expander Efficiency	60%	–
Feed Pump Efficiency	50%	–
Boiler Efficiency	90%	–
Rankine Cycle Mass Flow Rate	1.41 kg/s (typical)	Note: will vary

Before the two possible combined cycle setups can be compared it is necessary to come back to the concept of the maximum power point[38, 41]. That is, there is an optimal temperature for the exhaust to exit the high temperature heat exchanger which leads to maximum output from the TEG topping cycle. The hot side temperature of the TEG is dependent on the high temperature heat exchanger inlet and outlet temperatures (T_{HHi} and T_{HHo}). Like all heat engines, the power generated by the TEG will be dependent on the temperature difference across the device. A high T_{HHo} will lead to a high temperature ratio, and hence efficiency, but a low amount of heat removed from the exhaust stream (and passing through the TEG). A low T_{HHo} will result in a large amount of heat passing through the TEG but resulting in low conversion efficiency due to a low temperature ratio. This creates the optimum TE power condition as first pointed out by Hendricks and Lustbader [5] and amplified in Hendricks [31, 38] and Miller et al.[41].

For a set inlet temperature of 600 ^{o}C, Fig. 13 shows how the power generated in the combined cycle of Fig. 7 is affected by varying the hot side heat exchanger exit temperature (T_{HHo}). The TEG section and overall output clearly demonstrates the existence of a T_{HHo} value giving maximum power output. It is necessary to be aware of this system characteristic when comparing the two different combined cycle configurations shown in Figs. 6 and 7. The performance of each cycle will be compared at their own respective maximum power points for a given heat exchanger inlet temperature (T_{HHi}).

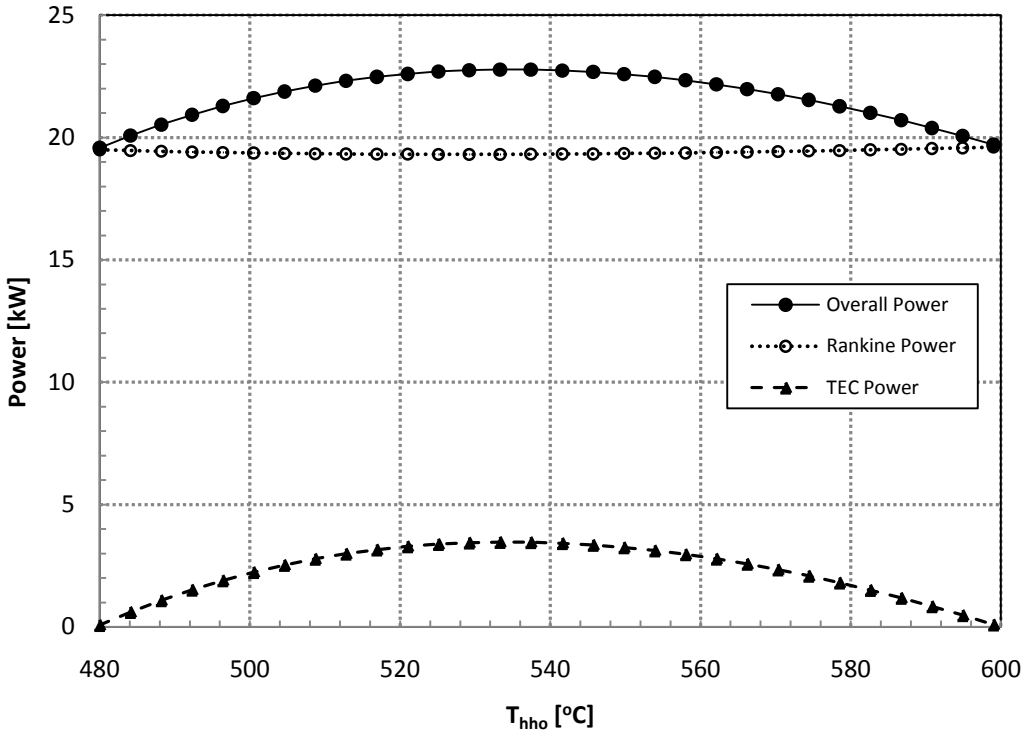

Figure 13: Power output of the R1 configuration at baseline conditions as a function of outlet temperature from the high temperature heat exchanger.

As T_{HHo} is swept from T_{HHi} to near the boiler temperature, the variation in overall power is due almost entirely to changes in the TEG power output as shown in Fig. 13. At low T_{HHo} values the TEG contributes almost nothing to the overall power. This is because the temperature drop across the TEG is low which leads to a low TEG efficiency. As T_{HHo} becomes higher the temperature drop across the TEG also increases so the efficiency of the TEG rises; this leads to improved generated power from the overall system. Eventually as T_{HHo} becomes near T_{HHi} only a small amount of heat is removed from the exhaust stream and the power developed by the TEG is low even though efficiency is high.

Maximizing the performance of the TEG will always result in maximized overall cycle power for a given set of ORC state points. This is because there is virtually no penalty on the ORC from the TEG topping cycle. Given the option of using the combined cycle or sending the sensible heat directly into the ORC, regardless of the TEG efficiency, the overall cycle will be more efficient with the combined cycle approach. Because the waste heat from the TEG goes into the ORC, the combined cycle approach is similar to an ORC-only cycle with a small amount of sensible heat removed and converted to electricity. The resulting effect is a loss of a small amount of heat input into the ORC equal to the electrical power generated in the TEG. Overall system power is increased because the ORC still sees greater than 90% of the heat passing through the TEG and nearly all of the sensible heat emerging from the high temperature heat exchanger. Thus, there is negligable apparent penalty for incorporating the TEG section into the combined cycle configuration.

Figure 14 presents a comparison of the three different configurations used to produce power from an exhaust stream having the baseline characteristics shown in Table 1. With the consideration that slightly different maximum power T_{HHo} values will exist for the R1 Fig.. 7 and A1Fig. 6 configurations, the figure shows the power output as a function of T_{HHi}, or the input temperature to the high temperature heat exchanger. All other parameters are held constant. Note that the Rankine only configuration (RO) shows the lowest power output over the range of inlet temperatures studied and there is no relevant T_{HHo} value for this case.

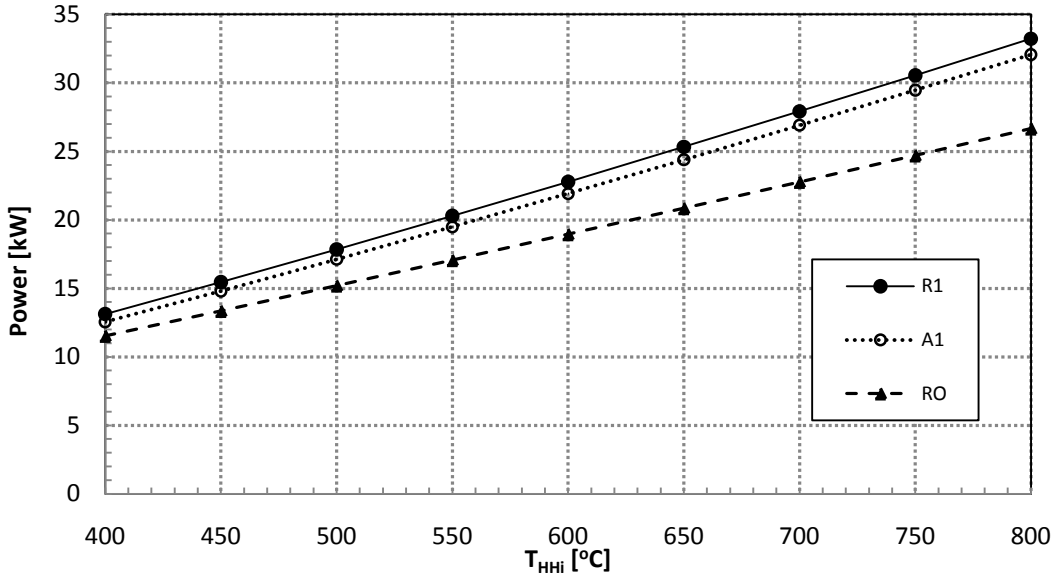

Figure 14:Comparison of the various configurations at their respective maximum power point for a range of inlet temperatures.

In Fig. 14 it is clear that the R1 configuration out performs the other two throughout the range of waste heat temperatures. Both configurations of the combined cycle, at their respective maximum power points, outperform the ORC only system. At a waste heat temperature of 673 K, the R1 configurations produces 13.9% more power than the ORC alone. At 1073 K the R1 configuration outperforms the ORC only configuration by 24.6%. As the temperature of the waste heat source increases, the temperature drop across the TEG increases which increases the efficiency of the TEG.

The performance gap increases between the ORC only and the combined cycles as the waste heat temperature increases because the efficiency of the combined cycle approach continues to increase while the efficiency of the ORC only cycle remains nearly constant. The temperature limitations of the ORC working fluid constrain the

upper temperature and limits the improvements in efficiency. The inability to significantly increase the efficiency of the ORC only configuration results in a nearly linear relationship between the waste heat temperature and the power output of the cycle.

Between the two combined cycle configurations, A1 and R1, the R1 configuration is superior to the A1 configuration throughout the range of waste heat temperatures. The difference is due to the capability of the exhaust and Rankine recuperators to transfer heat in the two different cases. In each case the recuperator in which the Rankine working fluid passes through first will increase the temperature of the Rankine working fluid and decrease the ability of the second recuperator to transfer heat. Because the specific heat of R245a is much greater than that of air, the Rankine recuperator is more sensitive to the cold side inlet temperature. Increasing this inlet temperature will reduce the performance of the Rankine recuperator more than the exhaust recuperator. Using the base line state points, the Rankine recuperator heat duty in the R1 configuration is 28.6 kW compared to 6.0 kW in the A1 configuration. This is because the Rankine recuperator's cold side inlet temperature in the R1 is lower.

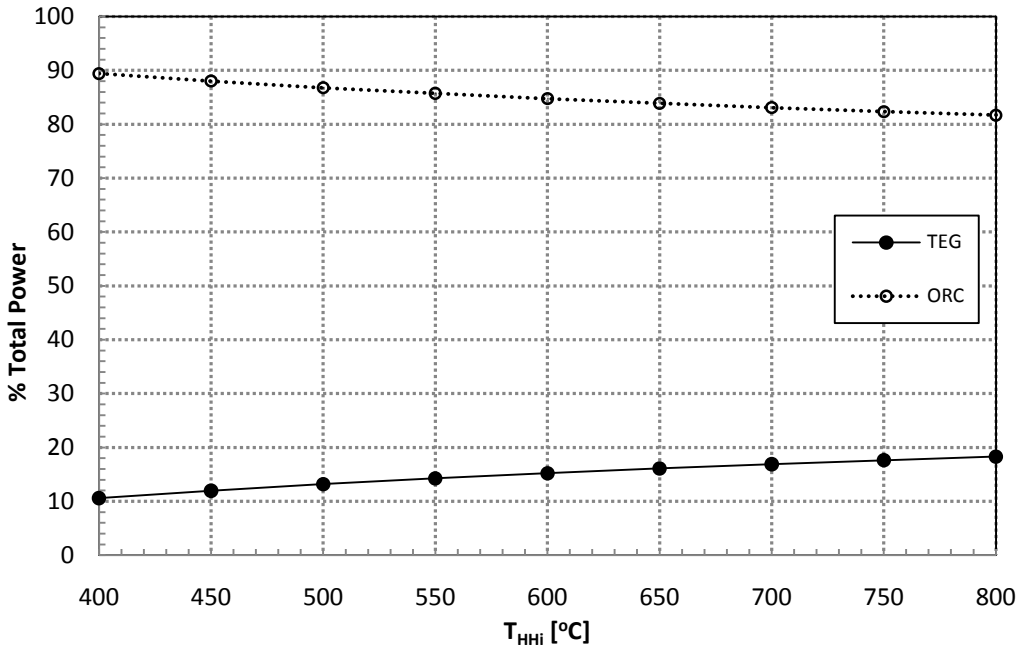

Figure 15: Power generated by the ORC and TEG sections of the dual cycle system (R1 configuration) as a function of inlet temperature.

Figure 15 compares the proportion of the power in the R1 configuration coming from the TEG with that from the ORC as T_{HHi} increases. The fraction of power generated from the TEG increases with T_{HHi} due to the growing amount of heat converted before the ORC. As noted, the efficiency of the TEG increases as the inlet temperature to the high temperature heat exchanger increases, thus a higher overall efficiency results. Efficiency in the ORC is governed by component efficiencies as well as the pressure ratio, amount of super heat and other parameters and is not as dependent on T_{HHi} , as was previously mentioned.

Figure 13 suggests that maximizing the performance of the TEG will give the highest performance for the combined cycle. However, the ORC still accounts for

over 80% of the overall power even at an exhaust temperature of 1072 K where the TEG is most effective. Hence maximizing the ORC output will ultimately have the larger effect on overall system performance. It must be kept in mind that most ORCs operating with one of the modern refrigerants (e.g. R245fa) has a maximum working fluid temperature between 210 to 230 ^{o}C, although for conservative operating conditions and ensuring no hot spots develop in the boiler, 200 ^{o}C is a better upper limit. So in cases where T_{HHi} is much higher than the ORC boiler temperature, having the TEG convert as much of the heat to electricity as possible is best, especially if the TEG material set can be matched to the temperature range of operation. This provides the combined cycle the capability to increase in efficiency due to higher temperatures which the ORC alone cannot accomplish. Within the above stated maximum upper temperature limit for ORC operation, methods for increasing the efficiency include adjusting the feed pump pressure ratio and the amount of super heat.

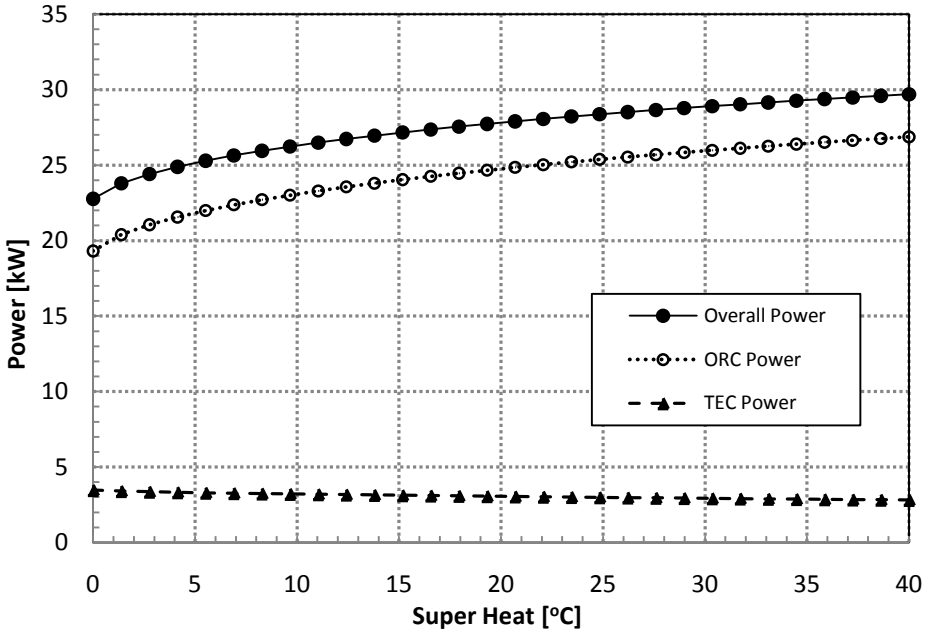

Figure 16: Power output as a function of ORC super heat for the R1 configuration.

At the nominal pressure ratio chosen for this analysis, Fig. 16 shows how the R1 configuration is affected by changing the amount of super heat. Increasing the level of this model parameter while holding the others constant provides significant improvement to the performance of the ORC. The output from the TEG suffers slightly but the overall system output increases significantly. Performance from the TEG degrades because as the working fluid in the ORC is heated to a higher temperature with the same amount of heat input, the ORC working fluid mass flow rate decreases. This causes a higher TEG heat rejection temperature in the pre-boiler. When the pre-boiler temperature increases, the cold side temperature of the TEG increases and the efficiency suffers due to a decrease in the ΔT across the TEG.

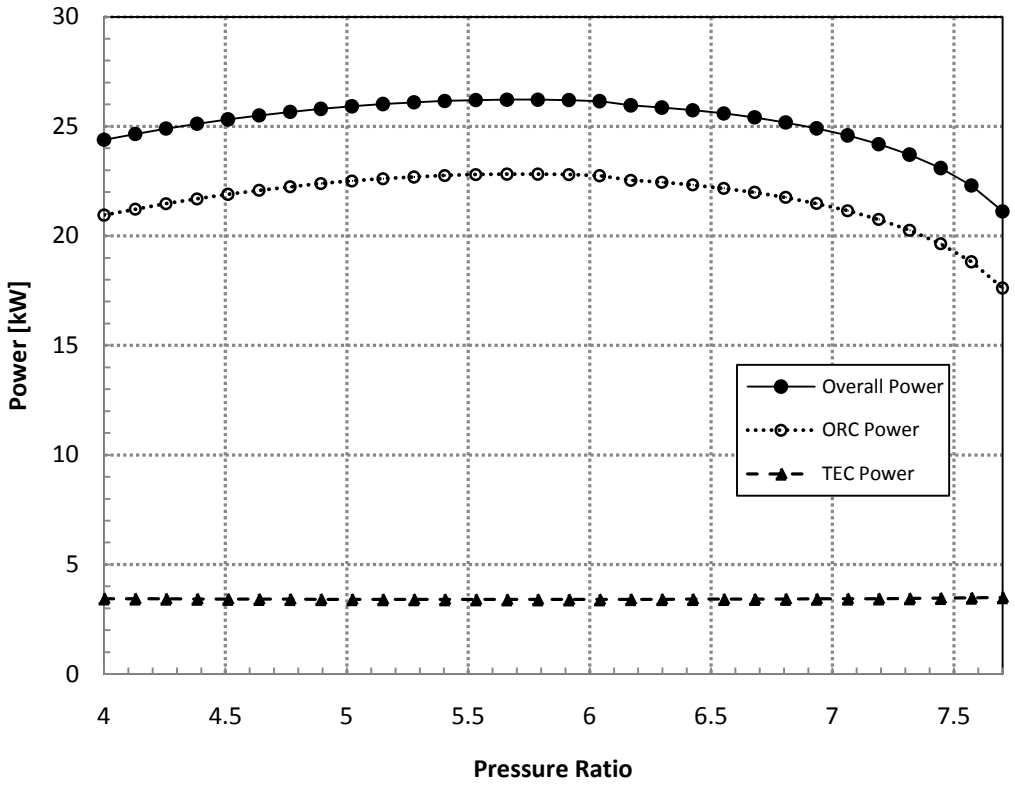

Figure 17: Effects of pressure ratio on power generated for the R1 configuration.

The effect of increasing the pressure ratio from 4 to 7.5 is dependent on the amount of super heat. Fig. 17 shows what the model predicts when increasing the pressure ratio and maintaining no super heat, i.e. the ORC working fluid exiting the boiler is at saturation conditions with a quality of 1 (given the boiler operating pressure). The power generated by the ORC increases until a pressure ratio of 5.75 is reached and then decreases thereafter. The TEG power is virtually unaffected. The reasoning for the precipitous decline in ORC output is explained in Fig. 18.

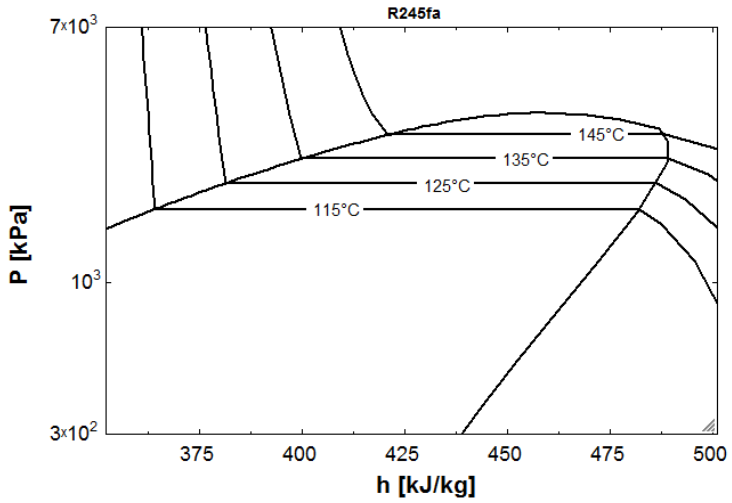

Figure 18: Pressure-Enthalpy diagram for R245fa showing the enthalpy behavior near the operating points of the ORC boiler.

With a pressure ratio of 7.5 in this model the maximum pressure in the ORC is 3475 kPa. The working fluid in this study, R245fa, has a critial pressure of 3639 kPa. Figure 18 shows the pressure vs enthalpy diagram for R245fa and explains that as the pressure increases the enthalpy will also increase to a point and then decreases. R245fa as a saturated vapor experiences a maximum enthalpy at a pressure of about 2800 kPa which in this model corresponds to a pressure ratio of 6. Introducing super heat, even small amounts (~5 ^{o}C), will eliminate the maxima at a pressure ratio of 6 and the cycle output power will continue to increase throughout the range of pressure ratios. Maximizing the enthalpy of the working fluid entering the boiler is important becaues the power generated by the expander is equal to the mass flow rate in the ORC multiplied by the change in enthalpy accros the expander.

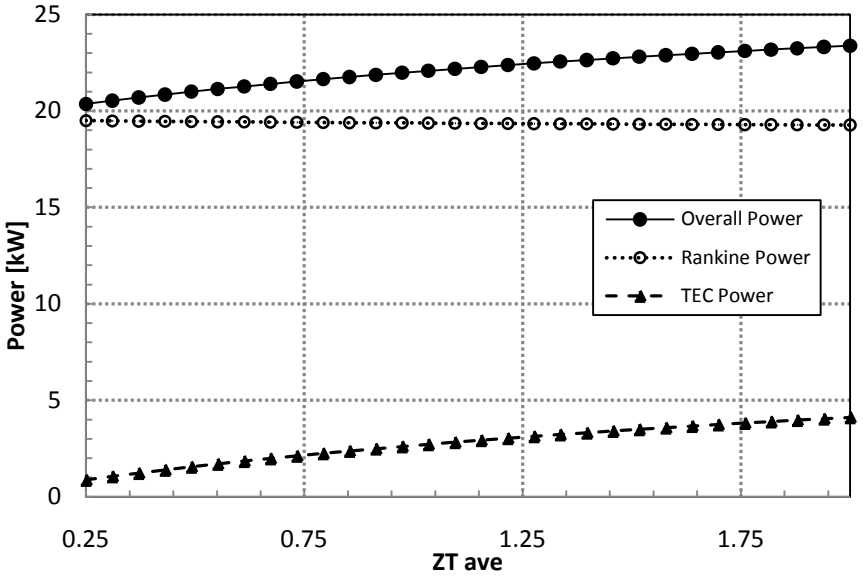

Figure 19: Power output as a function ZT_{ave} for the R1 configuration operating at baseline conditions except for the ZT_{ave} value.

Improving the TEG figure-of-merit through a variety of means including nano crystalline structure manipulation, use of lower dimensional configurations, development of skutterudites, nanocomposites, and quantum well structures are all contributing toward improving the *ZT* factor in TE materials. Fig. 19 shows how the combined cycle configuration R1 would benefit with an improved TEG according to this model given the baseline operating conditions and varying the ZT factor. It is not particularly surprising that Fig. 19 shows a steady improvement in TEG output with an increase in thermoelectric figure-of-merit. As more sensible heat is converted directly into electricity, less heat is available to power the ORC. The loss in ORC performance, however, is insignificant compared to the gain in power generated by the TEG.

6. Conclusions

This thesis presents modeling results from a study on two different combined cycle configurations for power generation using moderate-to-high grade waste heat. The combined cycles consist of a thermoelectric generator, which can utilize the higher temperature heat source, and an organic Rankine cycle to recover a large portion of the remaining energy. This work found that coupling a TEG to an ORC does not negatively affect the ORC because most of the heat powering the TEG finds its way eventually to the ORC. It is, however, important to operate the combined cycle at the maximum power point for the thermoelectric generator.

Although a small proportion of the power output is generated by the TEG, this power could play an important role in practical systems by operating the parasitic ORC system functions such as fans for the condenser and the motor for the feed pump. The TEG also is crucial because, while simultaneously producing useful power, it steps down the temperature at which heat is supplied to the ORC. This is an important factor in successful operation of the ORC in typical waste energy streams, as it effectively broadens the range of applications for ORC systems. The TEG also provides an avenue to higher cycle efficiencies at higher temperature not available to an ORC only system. With higher performing TE materials, potentially from the latest generation of advanced nano-based materials, additional power would be available for export outside the system. The characteristics of a baseline case were the focus of this work; however, preliminary results suggest that improving UA_h values and decreasing

the cold side heat rejection temperatures will be important considerations in future designs.

It should be noted that the purpose of this work has been to examine the potential benefits of adopting a combined cycle approach to waste heat recovery. As a result, the modeling of this cycle was idealized particularly in the area of losses. It was assumed that there was perfect heat transfer between components and no heat was lost to the surroundings. It was also assumed that there was no pressure drop in any of the ORC components. Any real cycle would have some amount of pressure drop and heat loss. The actual overall performance of the combined cycle presented in this work would certainly be lower than this idealized case. It is estimated that the power cycle would produce between 10 and 15% less power.

7. Next Steps

The future work in this area can be split into three main categories: more modeling work, experimental work and component improvement. A scaled down proof of concept system has been built and limited testing conducted. Continued work on this system will help to verify the mathematical model created in this study. It will also be a valuable learning tool in terms of evaluating the practicality of a small scale combined cycle.

Further modeling could be done in an attempt to optimize the combined cycle further. Specifically, it may be valuable to do a second law analysis of the system. The first law analysis accomplished in this work shows how energy is conserved throughout the system but does not show how the system can be improved. Second law analysis provides insight into where a system can be improved by showing where losses are taking place due to exergy destruction. Exergy destruction is a result of an increase in entropy in a component which, for example, can be a result of large temperature mismatch in a heat transfer component. Knowing where this is taking place will identify the “problem” areas of a cycle and allow for them to be addressed.

There will always be work in the field of waste heat recovery involving the improvement of system components. Highly efficient and compact. Light-weight components are a requirement if any system of this nature is going to be in the least bit practical. Size constraints dictate micro-channel components be used to achieve useful performance. It has also been shown that increasing the isentropic efficiency of the

vapor expander in a small scale vapor compression cycle can lead to large gains is system performance.

8. References

[1] Transportation Energy Data Book, 25th ed., 2002, U.S. Department of Energy, Office of Energy Efficiency and Renewable Energy, Oak Ridge National Laboratory, 2004.

[2] Annual Energy Review. U.S. Energy Information Administration. 2010. http://www.eia.doe.gov/aer/overview.html

[3] O. Bailey, E. Worrell, Clean Energy Technology A Preliminary Inventory of the Potential for Electricity Generation. Ernest Orlando Lawrence Berkeley National Laboratory, Environmental Energy Technoloies Division. 2005. http://www.recycled-energy.com/_documents/news/LBNL_clean_energy.pdf

[4] J. L. Pellegrino, N. Margolis, M. Justiniano, 2004, Energy Use, Loss, and Opportunity Analysis: U.S. Manufacturing and Mining, Energetics, Inc., Columbia, MD and E3M, Inc., North Potomac, MD.

[5] T.J. Hendricks, J.A. Lustbader, Advanced Thermoelectric Power System Investigations for Light-Duty and Heavy-Duty Vehicle Applications: Pat I, Proc. of the 21st International Conf. Thermoelectrics, IEEE Catalogue #02TH8657, (2002), pp. 381-386.

[6] R. B. Peterson, H. Wang, T. Herron, Performance of a small-scale regenerative Rankine power cycle employing a scroll expander, Power Energy, 222 (3), 271 – 282, (2008).

[7] S.G.K. Williams, D.M. Rowe, A. Kaliazin, Improved Thermoelectric Modules for Electrical Power Generation Using Low Temperature Waste Heat, Proc. 5th European Workshop Thermoelectrics (1999), pp. 93-98.

[8] M. S. Dresselhaus, G. Chen, M. Y. Tang, New Directions for Low-Dimensional Thermoelectric Materials, Adv. Mater. 19, 1043 (2007)

[9] G. S. Nolas, J. Poon, M. Kanatzidis, Recent Developments in Bulk Thermoelectric Materials, MRS Bulletin 31, 199 (2006)

[10] K. Matsuura, D. M. Rowe, Low-Temperature Heat Conversion, CRC Handbook of Thermoelectrics, D. M. Rowe, ed, (Boca Raton, FL: CRC, 1995), pp. 573 – 593.

[11] D.M. Rowe, G. Min, S.G,K. Williams, A. Aoune, K. Matsuura, V.L. Kuznetsov, and L. Fu, Thermoelectric Recovery of Waste heat – Case Studies, Proc.32nd International Energy Conversion Engineering Conf., Vol. 2, (1997), pp. 1075-1079.

[12] T. M. Tritt, M. A. Subramanian, Thermoelectric materials, phenomena, and applications: a bird's eye view, M.A., Materials Research Society Bulletin, 31, 3, 188, (Warrendale, PA: Materials Research Society, 2006)

[13] B. Poudel, Q. H. Hao, Y. Ma, High-Thermoelectric Performance of Nanostructured Bismuth Antimony Telluride Bulk Alloys, Sciencexpress, 10.1126, science.1156446, (2008)

[14] T. C. Hung, T.Y. Shai, S.K. Wang, A review of organic Rankine cycles (ORCs) for the recovery of low-grade waste heat, Energy, 22, 661 – 667, (1997)

[15] K.Y. Bronicki, A. Elovic, P. Rettger, Experience with organic Rankine cycles in heat recovery power plants, Proc. of the 58th American Power Conf., Part 2, (1996), pp. 1086 – 1089.

[16] Butcher C, Reddy B, Second law analysis of a waste heat recovery based power generation system, International Journal of Heat and Mass Transfer 50 (2007) 2355-2363

[17] Lee J, Kim T, Analysis of Design and Part Load Performance of Micro Gas Turbine/Organic Rankine Cycle Combined Systems, Journal of Mechanical Science and Technology, Vol. 20, No. 9, pp. 1502 ~ 1513, 2006

[18]Vaja I, Gambarotta A, Internal Combustion Engine (ICE) bottoming with Organic Rankine Cycles (ORCs), Energy (2009), doi:10.1016/j.energy.2009.06.001

[19] Danov S., Gupta A., Modeling the Performance Characteristics or Diesel Engine Based Combined-Cycle Power Plants—Part I: Mathematical Model, Engineering for Gas Turbines and Power (2004) Vol. 126

[20] Danov S, Gupta A, Modeling the Performance Characteristics or Diesel Engine Based Combined-Cycle Power Plants—Part II: Results and Applications, Engineering for Gas Turbines and Power (2004) Vol. 126

[21] Incropera F, Dewitt D, Bergman T, Lavine A, "Funamentals of Heat and Mass Transfer," Sixth Edition, New Jersey, Wiley, 2007

[22] Moran J, Shaoiro H, "Fundamentals of Engineering Thermodynamics," Fifth Edition, New Jersey, Wiley, 2006

[23] Thermodynamic Properties of Ammonia-Water Mixtures for Power Cycles. *International Journal of Thermophysics, Vol. 19, No. 2, 1998*

[24] Ibrahim O, Klein S, Absorption Power Cycles, Energy, Vol. 21, No. 1, pp 21-27, (1996)

[25] H, Mlcak, "An Introduction to the Kalina Cycle," Proceedings of the International Joint Power Generation Conference , PWR- Vol. 30, 1996

[26] First Law-based thermodynamic analysis on Kalina cycle. Energy Power Eng, 2008 2(2): 145-151

[27] U. Birkholz, "Conversion of Waste Exhaust Heat in Automobile using FeSi2 Thermoelements," *Proc. 7th Int. Conf. on Thermoelectrics* (Arlington, TX: University of Texas at Arlington, 1988), pp. 124–128.

[28] J. Fleurial, Thermoelectric Power generation materials: Technology and application opportunities, Journal of the Miners, metal and Materials Society, Vol. 61, 4, 79-85.

[29]T. Hendricks and W.T. Choate, *Engineering Scoping Study of Thermoelectric Generator Systems for Industrial Waste Heat recovery* (Washington, D.C.: Industrial Technologies Program, U.S. Department of Energy, 2006), pp. 1–76.

[30] K. Matsubara, "Development of a High Efficient Thermoelectric Stack for a Waste Exhaust Heat Recovery of Vehicles," *Proc. 21st Int. Conf. on Thermoelectrics* (Piscataway, NJ: IEEE, 2002), pp. 418–423

[31] T.J. Hendricks, Thermal System Interactions in Optimizing Advanced Thermoelectric Energy Recovery Systems, Energy Resources Technology, Vol. 129, No. 3, pp. 223-231, (2007).

[32] J. Horlock, Combined Power Plants – Past, Present, and Future, Trans of the ASME, J. of Engg, For Gas Turbine and Power, Vol 117, 1995.

[33] M. Briesch, R. Bannister, I. Diakunchak, D. Huber, "A Combined Cycle Designed to Achieve Greater Than 60 Percent Efficiency," Journal of engineering for gas turbines and power, Vol. 117, 1995

[34] R. Smith, P. Polukort, C. Maslak, C. Jones, B. Gardiner, "Advanced Technology Combined Cycles", GE Power Systems, GER-3936A, 2001.

[35]A. Bassily, "Modeling, numerical optimization, and irreversibility reduction of a triple-pressure reheat combined cycle," Energy 32 (2007) 778–794

[36] D. Sue, C, Chuang, "Engineering design and exergy analyses for combustion gas turbine based power generation systm", Energy, 29 (2004) pp. 1183-1205.

[37] M. Ghazikhani, M. Passandideh-Fard, M. Mousavi, 'Two new high-performance cycles for gas turbine with air bottoming", Energy (2010) pp. 1-11.

[38] T.J Hendricks, Microtechnology – A Key to System Miniaturization in Advanced Energy Recovery & Conversion Systems, ASME 2nd International Conf. Energy Sustainability (2008), Paper # ES2008-54244.

[39] R. Decher, "Direct Energy Conversion," (Oxford, England: Oxford University Press, 1997) pp. 240 – 252.

[40] S.W. Angrist, "Direct Energy Conversion," Fourth Edition, (Boston, MA: Allyn and Bacon, Inc., 1982) pp. 121 – 171.

[41] E. W. Miller, T. J. Hendricks, R. B. Peterson, "Modeling Energy Recovery Using Thermoelectric Conversion Integrated with an Organic Rankine Bottoming Cycle", Journal of Electronic Materials, 38(7): 1206-1213.

9. Appendices

9.1 Computational Code

```
PROCEDURE
Q_RECUPERankine(PWF$,T_Ci,T_Hi,P_c,P_h,h_Hi,h_Ci:Q_rec_spec,Marker)
 T_sat,h := T_sat ( PWF$ , P = P_h )
 Q_rec,specC := h ( PWF$ , T = T_Hi , P = P_c ) – h_Ci
 If ( ( T_Ci < T_sat,h ) or ( T_Ci = T_sat,h ) ) Then
 Q := h ( PWF$ , T = T_sat,h , P = P_c ) – h_Ci
 h_min := h ( PWF$ , P = P_h , x = 1 ) – Q
 Q_rec,specH := h_Hi – h_min
 If ( ( Q_rec,specH > Q_rec,specC ) or ( Q_rec,specH = Q_rec,specC ) ) Then
 Q_rec,spec := Q_rec,specC
 Q_rec,spec := Q_rec,specH
 EndIf
 Marker := 1
 Q_rec,spec := h_Hi – h ( PWF$ , P = P_h , T = T_Ci )
 Marker := 0
End Q_RECUPERankine

 ṁ_air = 0.5 [kg/s]
 T_HHi = 600 [C]
 T_HHo = 535 [C]
 T_amb = 40 [C]
 Heat_req = ṁ_air · ( h_HHi – h ( 'Air' , T = T_amb ) )
 n = 1
 UA = 0.3
 UAs = UA
 zt = 1.5
 Resistance_H = 1.5
 Resistance_L = 1.5
 Heatloss_HS = 0
 Heatloss_LS = 0
 PWF$ = 'R245fa'
 CWF$ = 'R134a'
 T_evap = 11 [C]
 T_cond,P = 60 [C]
 T_cond,C = 50 [C]
```

$Superheat_C = 5$ [C]

$Subcool_P = 4$ [C]

$Subcool_C = 10$ [C]

$Eff_p = 0.5$

$Eff_c = 0.75$

$Eff_{exp} = 0.6$

$Eff_{re,r} = 0.8$

$Eff_{re,ex} = 0.8$

$Eff_{boiler} = 0.9$

$PD_{heatexchanger} = 0$

$PD_{preboiler} = 0$

$PD_{boiler,r} = 0$

$PD_{boiler,a} = 0$

$PD_{recupe,r,hot} = 0$

$PD_{recupe,r,cold} = 0$

$PD_{recupe,ex,air} = 0$

$PD_{recupe,ex,r} = 0$

$PD_{condenser,p} = 0$

$PD_{condenser,c} = 0$

$PD_{evap} = 0$

$Kc = 273.15$

$h_{HHi} = \mathbf{h}('Air', T = T_{HHi})$

$h_{HHo} = \mathbf{h}('Air', T = T_{HHo})$

$X_i = i \quad \text{for } i = 1 \text{ to } n$

$mdotcp_i = \dot{m}_{air} \cdot \mathbf{Cp}('Air', T = T_{ave,h,i}) \quad \text{for } i = 1 \text{ to } n$

$$T_{HHis,i} = T_{HHi} - \left[(T_{HHi} - T_{HHo}) \cdot \left(\frac{2 \cdot X_i - 2}{2 \cdot n} \right) \right] \quad \text{for } i = 1 \text{ to } n$$

$$T_{HHos,i} = T_{HHi} - (T_{HHi} - T_{HHo}) \cdot \frac{2 \cdot X_i}{2 \cdot n} \quad \text{for } i = 1 \text{ to } n$$

$$T_{ave,h,i} = T_{HHi} - \left[(T_{HHi} - T_{HHo}) \cdot \left(\frac{2 \cdot X_i - 1}{2 \cdot n} \right) \right] \quad \text{for } i = 1 \text{ to } n$$

$$EXPHH_i = \mathbf{exp}\left[\frac{-UAs}{mdotcp_i} \right] \quad \text{for } i = 1 \text{ to } n$$

$e_i = 1 - EXPHH_i \quad \text{for } i = 1 \text{ to } n$

$$e_i = \frac{T_{HHis,i} - T_{HHos,i}}{T_{HHis,i} - T_{HHs,i}} \quad \text{for } i = 1 \text{ to } n$$

$Q_{H,i} = mdotcp_i \cdot e_i \cdot (T_{HHis,i} - T_{HHs,i}) \quad \text{for } i = 1 \text{ to } n$

$$Q_{Ha,i} = Q_{H,i} \cdot (1 - Heatloss_{HS}) \quad \text{for } i = 1 \text{ to } n$$

$$\square_{T,H,i} = Q_{H,i} \cdot Resistance_{H} \quad \text{for } i = 1 \text{ to } n$$

$$\square_{T,L,i} = Q_{L,i} \cdot Resistance_{L} \quad \text{for } i = 1 \text{ to } n$$

$$\square_{T,H,i} = T_{HHs,i} - T_{HX,i} \quad \text{for } i = 1 \text{ to } n$$

$$T_{ave,i} = \frac{Kc + T_{HX,i} + Kc + T_{LX,i}}{2} \quad \text{for } i = 1 \text{ to } n$$

$$z_i \cdot T_{ave,i} = zt \quad \text{for } i = 1 \text{ to } n$$

$$T_{ratio,i} = \frac{Kc + T_{HX,i}}{Kc + T_{LX,i}} \quad \text{for } i = 1 \text{ to } n$$

$$M_{opt,i} = \left[1 + z_i \cdot \left(\frac{Kc + T_{HX,i} + Kc + T_{LX,i}}{2}\right)\right]^{(1/2)} \quad \text{for } i = 1 \text{ to } n$$

$$Eff_{TEC,i} = \left[\frac{T_{HX,i} + Kc - (Kc + T_{LX,i})}{T_{HX,i} + Kc}\right] \cdot \left[\frac{M_{opt,i} - 1}{M_{opt,i} + \frac{Kc + T_{LX,i}}{Kc + T_{HX,i}}}\right] \quad \text{for } i = 1 \text{ to } n$$

$$Carnot_{eff,i} = 1 - \left[\frac{Kc + T_{LX,i}}{Kc + T_{HX,i}}\right] \quad \text{for } i = 1 \text{ to } n$$

$$Q_{Ha,i} - Q_{L,i} = W_{out,TEC,i} \quad \text{for } i = 1 \text{ to } n$$

$$W_{out,TEC,i} = Eff_{TEC,i} \cdot Q_{Ha,i} \quad \text{for } i = 1 \text{ to } n$$

$$T_{LXX,j} = T_{LX,j} \quad \text{for } j = 1 \text{ to } n$$

$$W_{out,TEC,T} = \sum_{i=1}^{n} (W_{out,TEC,i})$$

$$Q_{H,T} = \sum_{i=1}^{n} (Q_{H,i})$$

$$Q_{L,T} = \sum_{i=1}^{n} (Q_{L,i})$$

$$Q_{Ha,T} = \sum_{i=1}^{n} (Q_{Ha,i})$$

$$XX_k = k \quad \text{for } k = 1 \text{ to } n$$

$$Q_{L,s,k} = \sum_{i=1}^{k} (Q_{L,i}) \quad \text{for } k = 1 \text{ to } n$$

$$Q_{L,s,k} \cdot (1 - Heatloss_{LS}) = \dot{m}_r \cdot (h_{8,k} - h_7) \quad \text{for } k = 1 \text{ to } n$$

$$P_{8,k} = P_7 - PD_{preboiler} \cdot XX_k \quad \text{for } k = 1 \text{ to } n$$

$$x_{8,k} = \mathbf{x}(PWF\$, h = h_{8,k}, P = P_{8,k}) \quad \text{for } k = 1 \text{ to } n$$

$$T_{8,k} = \mathbf{T}(PWF\$, h = h_{8,k}, P = P_{8,k}) \quad \text{for } k = 1 \text{ to } n$$

$$T_{L,k} = T_{8,k} \quad \text{for } k = 1 \text{ to } n$$

$\square_{T,L,k} = T_{LXX,k} - T_{L,k}$ for $k = 1$ to n

$h_{air,exhaust,1} = \mathbf{h}('Air', T = T_{air,exhaust,1})$

$Q_{rec,air} = \dot{m}_{air} \cdot (h_{HHo} - \mathbf{h}('Air', T = T_{8,1}))$

$Q_{in,boiler} = Q_{rec,air} \cdot Eff_{boiler}$

$Q_{in,boiler} = \dot{m}_{air} \cdot (h_{HHo} - h_{air,exhaust,1})$

$Q_{L,T} \cdot (1 - Heatloss_{LS}) + Q_{in,boiler} = \dot{m}_r \cdot (h_1 - h_7)$

$P_{cond,P} = \mathbf{P}_{sat}(PWF\$, T = T_{cond,P})$

$P_{Pump} = P_{ratio} \cdot P_{cond,P}$

$h_{sat,liq} = \mathbf{h}(PWF\$, P = P_1, x = 0)$

$h_{sat,vap} = \mathbf{h}(PWF\$, P = P_1, x = 1)$

$scroll_{vol,exp} = 0.0000075$

$P_1 = P_{8,1} - PD_{boiler,r}$

$T_{sat1} = \mathbf{T}_{sat}(PWF\$, P = P_1)$

$T_1 = T_{sat1} + SuperHeat_P$

$h_1 = \mathbf{h}(PWF\$, T = T_1, P = P_1)$

$s_1 = \mathbf{s}(PWF\$, T = T_1, P = P_1)$

$x_1 = \mathbf{x}(PWF\$, h = h_1, P = P_1)$

$\square_1 = \square(PWF\$, T = T_1, P = P_1)$

$$\square_1 \cdot scroll_{vol,exp} \cdot \frac{rpm_{exp}}{60} = \dot{m}_r$$

$p_2 = P_3 + PD_{recupe,r,hot}$

$s_{2s} = s_1$

$h_{2s} = \mathbf{h}(PWF\$, s = s_{2s}, P = p_2)$

$h_2 = h_1 - Eff_{exp} \cdot (h_1 - h_{2s})$

$T_2 = \mathbf{T}(PWF\$, h = h_2, P = p_2)$

$x_2 = \mathbf{x}(PWF\$, h = h_2, P = p_2)$

Call $\mathbf{Q}_{RECUPERankine}(PWF\$, T_5, T_2, P_6, P_3, h_2, h_5 : Q_{rec,r,spec}, Marker)$

$Q_{rec,r,spec} \cdot Eff_{re,r} \cdot \dot{m}_r = Q_{recupe,r}$

$h_{2o} = \mathbf{h}(PWF\$, P = P_3, x = 1)$

$Q_{check,r} = \dot{m}_r \cdot (h_2 - h_{2o})$

$Q_{check,r} = \dot{m}_r \cdot (h_6 - \mathbf{h}(PWF\$, T = T_{5o}, P = P_6))$

$T_{pinch,r} = T_{cond,P} - T_{5o}$

$P_3 = P_{cond,P} + PD_{condenser,p}$

$P_6 = P_5 - PD_{recupe,r,cold}$

$Q_{recupe,r} = \dot{m}_r \cdot (h_2 - h_3)$

$Q_{recupe,r} = \dot{m}_r \cdot (h_6 - h_5)$

$T_3 = \mathbf{T}(PWF\$, h = h_3, P = P_3)$

$$x_3 = \mathbf{x}(PWF\$, P = P_3, h = h_3)$$

$$T_6 = \mathbf{T}(PWF\$, h = h_6, P = P_6)$$

$$x_6 = \mathbf{x}(PWF\$, P = P_6, h = h_6)$$

$$T_4 = T_{cond,P} - Subcool_P$$

$$h_4 = \mathbf{h}(PWF\$, P = P_{cond,P}, T = T_4)$$

$$s_4 = \mathbf{s}(PWF\$, P = P_{cond,P}, T = T_4)$$

$$Q_{cond,p} = \dot{m}_r \cdot (h_3 - h_4)$$

$$P_5 = P_{Pump}$$

$$s_{5s} = s_4$$

$$h_{5s} = \mathbf{h}(PWF\$, s = s_{5s}, P = P_5)$$

$$h_5 = h_4 + \frac{1}{Eff_p} \cdot (h_{5s} - h_4)$$

$$T_5 = \mathbf{T}(PWF\$, h = h_5, P = P_5)$$

$$s_5 = \mathbf{s}(PWF\$, T = T_5, P = P_5)$$

$$x_5 = \mathbf{x}(PWF\$, h = h_5, P = P_5)$$

$$P_7 = P_6 - PD_{recupe,ex,r}$$

$$Q_{rec,ex,h} = \dot{m}_{air} \cdot (h_{air,exhaust,1} - \mathbf{h}('Air', T = T_6))$$

$$Q_{recupe,ex} = Q_{rec,ex,h} \cdot Eff_{re,ex}$$

$$Q_{recupe,ex} = \dot{m}_r \cdot (h_7 - h_6)$$

$$Q_{recupe,ex} = \dot{m}_{air} \cdot (h_{air,exhaust,1} - h_{air,exhaust,2})$$

$$T_{air,exhaust,2} = \mathbf{T}('Air', h = h_{air,exhaust,2})$$

$$T_7 = \mathbf{T}(PWF\$, h = h_7, P = P_7)$$

$$x_7 = \mathbf{x}(PWF\$, P = P_7, h = h_7)$$

$$\dot{m}_r \cdot (\mathbf{h}('R245fa', P = P_7, x = 0) - h_7) = \dot{m}_{air} \cdot (\mathbf{h}('Air', T = T_{check1}) - h_{air,exhaust,1})$$

$$T_{R245fa1} = \mathbf{T}_{sat}('R245fa', P = P_7)$$

$$pinch = T_{check1} - T_{R245fa1}$$

$$w_{exp} = \dot{m}_r \cdot (h_1 - h_2)$$

$$w_{pump} = \dot{m}_r \cdot (h_5 - h_4)$$

$$w_r = w_{exp} - w_{pump}$$

$$Q_{in,rankine,r} = \dot{m}_{air} \cdot (h_{HHo} - h_{air,exhaust,2}) + \sum_{i=1}^{n} (Q_{L,i}) \cdot (1 - Heatloss_{LS}) + Q_{recupe,r}$$

$$Q_{in,rankine} = \dot{m}_{air} \cdot (h_{HHo} - h_{air,exhaust,2}) + \sum_{i=1}^{n} (Q_{L,i}) \cdot (1 - Heatloss_{LS})$$

$$Eff_{rankine} = \frac{w_r}{Q_{in,rankine}}$$

$$w_{exp} = w_{comp} + w_{pump}$$

$$P_{cond,C} = \mathbf{P}_{sat}(CWF\$, T = T_{cond,C})$$

$$P_{ratio,comp} = \frac{P_{cond,C}}{P_{evap}}$$

$$P_{evap} = \mathbf{P}_{sat}(CWF\$, T = T_{evap})$$

$$scroll_{vol,comp} = scroll_{vol,exp} \cdot 0.8$$

$$P_{C11} = P_{cond,C}$$

$$T_{C11} = T_{cond,C} - Subcool_C$$

$$h_{C11} = \mathbf{h}(CWF\$, T = T_{C11}, P = P_{C11})$$

$$s_{C11} = \mathbf{s}(CWF\$, T = T_{C11}, P = P_{C11})$$

$$h_{C11} = h_{C22}$$

$$P_{C22} = P_{evap} + PD_{evap}$$

$$x_{C22} = \mathbf{x}(CWF\$, h = h_{C22}, P = P_{C22})$$

$$T_{C33} = T_{evap} + Superheat_C$$

$$P_{C33} = P_{evap}$$

$$h_{C33} = \mathbf{h}(CWF\$, T = T_{C33}, P = P_{C33})$$

$$s_{C33} = \mathbf{s}(CWF\$, T = T_{C33}, P = P_{C33})$$

$$\square_{C33} = \square(CWF\$, T = T_{C33}, P = P_{C33})$$

$$\square_{C33} \cdot scroll_{vol,comp} \cdot \frac{rpm_{comp}}{60} = \dot{m}_c$$

$$T_{C44} = T_{cond,C}$$

$$s_{C44s} = s_{C33}$$

$$P_{C44} = \mathbf{P}_{sat}(CWF\$, T = T_{cond,C})$$

$$h_{C44s} = \mathbf{h}(CWF\$, s = s_{C44s}, P = P_{C44})$$

$$h_{C44} = h_{C33} + \frac{1}{Eff_c} \cdot (h_{C44s} - h_{C33})$$

$$w_{comp} = \dot{m}_c \cdot (h_{C44} - h_{C33})$$

$$Q_{cond,C} = \dot{m}_c \cdot (h_{C44} - h_{C11})$$

$$Q_{cooling} = \dot{m}_c \cdot (h_{C33} - h_{C22})$$

$$COP_{cooling} = \frac{Q_{cooling}}{w_{comp}}$$

$$Q_{in,total} = \dot{m}_{air} \cdot (h_{HHi} - h_{air,exhaust,2})$$

$$W_{overall} = W_{out,TEC,T} + w_r$$

$$Eff_{overall} = \frac{W_{overall}}{Q_{in,total}}$$

$$Eff_{actual} = \frac{W_{overall}}{\dot{m}_{air} \cdot (h_{HHi} - \mathbf{h}('Air', T = T_{amb}))}$$

$$T_{TE,Drop} = T_{HX,1} - T_{LX,1}$$

$$RPM_{ratio,comp} = \frac{rpm_{comp}}{rpm_{exp}}$$

$$RPM_{ratio,exp} = \frac{1}{RPM_{ratio,comp}}$$